Inorganica Chimica Acta 525 (2021) 120486

Contents lists available at ScienceDirect

Inorganica Chimica Acta

journal homepage: www.elsevier.com/locate/ica

Research paper

Silver (I)-*N*-heterocyclic carbene complexes: Synthesis and characterization, biological evaluation of Anti-Cholinesterase, anti-alpha-amylase, anti-lipase, and antibacterial activities, and molecular docking study

Abd El-Krim Sandeli [a,c], Naima Khiri-Meribout [a,*], Saida Benzerka [a], Nevin Gürbüz [b,c], Muhammed Dündar [d], Hüseyin Karcı [e], Chawki Bensouici [f], El Hassen Mokrani [g], İlknur Özdemir [b], Ahmet Koç [h], Namık Özdemir [i], Abdelmadjid Debache [a], İsmail Özdemir [b,c,*]

[a] *Laboratory of Synthesis of Molecules with Biological Interest, Faculty of Exact Sciences, Brother's Mentouri Constantine 1 University, 25000 Constantine, Algeria*
[b] *Faculty of Science and Art, Department of Chemistry, İnönü University, Malatya, Turkey*
[c] *Catalysis Research and Application Center, İnönü University, 44280 Malatya, Turkey*
[d] *Faculty of Medicine, Department of the Medical Biology and Genetics, İnönü University, Malatya, Turkey*
[e] *Medical School, Department of Medical Biology and Genetics, İnönü University, Battalgazi, Malatya, Turkey*
[f] *National Center for Biotechnologie Research (CRBt), Ali Mendjli New Town, Constantine, Algeria*
[g] *Laboratory of Applied Biochemistry, Department of Biochemistry and Cellular and Molecular Biology, Faculty of Natural and Life Sciences, Brother's Mentouri Constantine 1 University, Constantine, Algeria*
[h] *Inonu University, Medical School, Department Genetics, Battalgazi, Malatya, Turkey*
[i] *Department of Mathematics and Science Education, Faculty of Education, Ondokuz Mayıs University, 55139 Samsun, Turkey*

ARTICLE INFO

Dedicated to Professor Christian Bruneau

Keywords:
Silver(I)–NHC complexes
Antimicrobial
Anticholinesterase activity (*anti*-Alzheimer)
Anti-lipase activity
Anti-diabetic activity
X-Ray
Molecular docking

ABSTRACT

A series of novel silver(I)-*N*-heterocyclic carbene complexes have been prepared and fully characterized by spectroscopic methods and X-ray crystallographic analyses. The biological capacity of the synthesized compounds was evaluated *in vitro* for their anti-microbial, anti-cholinesterase, anti-lipase, anti-diabetic activities in search of potent inhibitors compound. All compounds were tested against two types of fungi and three bacterias. The results proved that most compounds indicated moderate to excellent activity against all types of bacteria and fungi except compound **2f** that didn't show any antibacterial activity. The synthesized compound's capacity to inhibit the enzymes AChE, BChE, Lipase, and α-amylase were evaluated. The results showed that silver(I)–NHC complexes **3a-f** are effective against all types of enzymes. The highest activity was reported toward AChE, BChE, and α-amylase enzymes, and at a lower rate against Lipase enzyme compared to the references drug. In contrast, benzimidazolium salts **2a-f,** which showed significant inhibitory activity against AChE and BChE enzymes, while all salts were not active against both Lipase and α-amylase enzymes. Molecular docking simulations using AutoDock, have been performed of the new compounds as a representative set of our molecules into AChE and BChE enzymes for lead optimization of the binding interaction template of the most active inhibitors docked into the active site of their relevant AChE and BChE enzymes inhibitors.

1. Introduction

The chemistry of *N*-heterocyclic carbenes (NHCs) has appeared as flexible building blocks for the ligation of a large variety of coordination compounds[1]. It has limited to metal coordination compounds derived from benzimidazolium precursors. Recently, *N*-Heterocyclic Carbenes' use in organometallic chemistry as ligands pulled insignificant consideration and became a rapidly growing field with a broad range of

Abbreviations: **NHC**, *N*-Heterocyclic carbine; **NMR**, Nucleare Magnetic Resonance; **IR**, Infrared spectra; **DMSO**, Dimethyl sulfoxide; **Ag_2O**, Silver oxide; **AChE**, Acetylcholinesterase; **BChE**, Butyrylcholinesterase; ***p*-NPP**, *p*-Nitrophenol Palmitate; **MIC**, Minimum Inhibitory Concentration; **CAS**, Catalytic anionic site; **PAS**, Peripheral anionic site.

* Corresponding authors at: Faculty of Science and Art, Department of Chemistry, İnönü University, Malatya, Turkey (İ. Özdemir). Laboratory of Synthesis of Molecules with Biological Interest, Faculty of Exact Sciences, Brother's Mentouri Constantine 1 University, 25000 CONSTANTINE, ALGERIA (N. Khiri-Meribout).

https://doi.org/10.1016/j.ica.2021.120486
Received 23 March 2021; Received in revised form 9 May 2021; Accepted 29 May 2021
Available online 2 June 2021

medicinal applications [2]. Currently, as a new emerging field of chemistry and medicinal research, metal-*N*-heterocycle carbenes (M-NHC) complexes have strongly appeared, where NHC complexes with different metals as (Cu, Au and Ag) proved to be active against several types of diseases as anticancer agents[3-7]. Among different transition metal-*N*-heterocyclic carbene complexes, the use of NHC with silver metal is the more important M-NHC−complexes, it has extraordinary consideration because of their structures, now has been broadly used as sources of different metal complexes in organic chemistry as transfer agents in the reaction of transmetalation due to the effective carbene, that allowed to form other NHC-metal complexes. Besides, the low silver toxicity for humans has attracted the researcher's attention to explore their biological activity and their medical applications, specifically antimicrobial and anticancer [1,8,9]. The synthesis of silver(I) complexes is generally done according to a straightforward procedure listed in the literature, starting from benzimidazolium salts or using directly commercial *N*-heterocycle carbenes [10-14]. In general, the *N*-heterocyclic carbenes (NHCs) could be generated by deprotonation of the related benzimidazolium salts. Our experience led us directly to adopt these types of complexes using 3,5-dimethylbenzimidazolium salts, which consider as very reactive ligands. However, most literature methods showed that the preparation of the silver(I)–NHC complexes have generally based on *N*-alkylation reactions to synthesis benzimidazolium salts as a precursor to nucleophilic carbenes. This type of ligands' characteristic was considered a strong σ donor property, which confirms that benzimidazolium salts are stronger than alkyl phosphines ligand and even the steric properties are also different than phosphines. In many cases, these properties and advantages frequently lead to greater stability of the catalysts[15-17]. On the other hand, benzimidazole salts are an important class that attracted considerable attention in various chemical, biological and industrial areas [18]. Further, the family of *N*-heterocyclic carbenes (NHCs) possessing a wide range of biological activities [3]. The coupling of these two types of compounds generates a pharmaceutically enhanced class of compounds known as M-NHC complexes.

As part of our ongoing research into novel functionalized NHC ligands as supporting a favorable environment for the development and application of metal complexes, Herein, we report the preparation of a new series of silver(I)–NHC complexes that contain 5,6-dimethylbenzimidazole. All the new products are tested against different biological activities such as anti-microbial, anti-Alzheimer, anti-lipase, and anti-diabetic. Also, to recognize and validate the inhibition mechanisms, a molecular docking analysis was carried out.

2. Experimental

2.1. Chemistry

2.1.1. Materials and methods

All reactions for the preparation of the benzimidazolium salts and their complexes Ag(I)–NHC were carried out under argon in flame-dried glassware using standard Schlenk techniques. All reagents were purchased from Sigma-Aldrich, Merck, and Fluka. ^{1}H NMR and ^{13}C NMR spectra were recorded with a Varian As 400 Merkur spectrometer operating at 400 MHz (^{1}H), 100 MHz (^{13}C) in $CDCl_3$ with tetramethylsilane as an internal reference. Coupling constants (*J* values) are given in Hertz. NMR multiplicities are abbreviated as follows: *s* = singlet, *d* = doublet, *t* = triplet, *sept* = septet, *q* = quartet and *m* = multiplet signal. FT-IR spectra were recorded on the ATR unit in the range 400–4000 cm^{-1} on Perkin Elmer Spectrum 100. Melting points were measured in open capillary tubes with Stuart SMP 40 melting point apparatus and uncorrected. Elemental analyses were performed at the İnönü University research center.

2.1.2. General procedure for the preparation of benzimidazolium salts (2a-f)

The benzimidazolium salts can be prepared in analogy to published procedures according to a slightly modified procedure from the literature methods [19]. A mixture of 1-benzyl-5,6-dimethylbenzimidazole (1 mmol) and an equivalent amount of alkyl halide derivative (1 mmol), in degassed dimethylformamide, was heated and stirred at 80 °C for 48 h under argon. The obtained mixture was cooled at room temperature. After 45 mL of ether were added and stirred for 1 h, then the product filtered and washed with diethyl ether to remove the impurities, and the product was left precipitated with high purity. After, the crude products were recrystallized in dichloromethane/diethyl ether and dried under vacuum to provide pure products for experimental analysis.

1-Benzhydryl −5,6-dimethyl-(2,3,5,6-tetramethylbenzyl)benzimidazolium chloride (2a)

Yield 85% (421 mg, white solid); m.p = 152–153 °C; FT-IR $\nu_{(CN)}$ = 1549 cm^{-1} .^{1}H NMR (400 MHz, $CDCl_3$, TMS, 25 °C): δ (ppm) = 10.45 (s, 1H, NC<u>H</u>N); 7.62 (s, 1H, N-$C_6\underline{H}_2(CH_3)_2$-N); 7.38–7.36 (m, 6H, C<u>H</u>-Ar); 7.34–7.30 (m, 4H, C<u>H</u>-Ar); 7.01 (s, 1H, N-$C_6\underline{H}_2(CH_3)_2$-N); 6.93 (s, 1H, Ph-C<u>H</u>-Ph); 5.90 (s, 2H, $C\underline{H}_2$N); 2.23 (s, 3H, $C\underline{H}_3$); 2.21 (s, 6H, $C\underline{H}_3$); 2.19 (s, 9H, $C\underline{H}_3$). ^{13}C NMR (400 MHz, $CDCl_3$, TMS, 25 °C): δ (ppm) = 142.3 (N<u>C</u>HN,C_1); 137.0 (C_4); 136.9 (C_6); 135.7 ($C_{22,28}$); 134.9 ($C_{14,17}$); 134.0 ($C_{12,19}$); 133.3 (C_{11}); 130.6 (C_2); 130.0 (C_9); 129.3 (4<u>C</u>H, $C_{24,26,30,32}$); 129.2 (2<u>C</u>H, $C_{25,31}$); 128.4 (4<u>C</u>H, $C_{23,27,29,33}$); 128.1 (<u>C</u>H, C_{16}); 114.6 (<u>C</u>H, C_3); 113.6 (<u>C</u>H, C_8); 66.1 (<u>C</u>H, C_{21}); 47.9 (N-<u>C</u>H_2, C_{10}); 20.8 (2<u>C</u>H_3, $C_{15,18}$); 20.7 (CH_3, C_7); 20.5 (<u>C</u>H_3, C_5); 16.1 (2<u>C</u>H_3, $C_{13,20}$). Elemental analysis calcd. (%) for $C_{33}H_{36}ClN_2$ (M.w. = 496.11 g/mol): C 79.89, H 7.31, N 5.65; found (%): C 79.83, H 6.78, N 5.35

1-Benzhydryl −5,6-dimethyl-(4-methylbenzyl)benzimidazolium chloride (2b)

Yield 71% (322 mg, white solid); m.p = 159–160 °C; FT-IR $\nu_{(CN)}$ = 1548 cm^{-1}. ^{1}H NMR (400 MHz, $CDCl_3$, TMS, 25 °C): δ (ppm) = 11.27 (s, 1H, NC<u>H</u>N); 7.37 (d, *J* = 5.7 Hz, 6H, C<u>H</u>-Ar); 7.34 (s, 3H, C<u>H</u>-Ar); 7.32 (s, 2H, C<u>H</u>-Ar); 7.29 (s, 2H, C<u>H</u>-Ar); 7.11 (d, *J* = 7.2 Hz, 2H, C<u>H</u>-Ar); 6.97 (s, 1H, Ph-C<u>H</u>-Ph); 5.84 (s, 2H, $C\underline{H}_2$N); 2.28 (s, 3H, $C\underline{H}_3$); 2.27 (S, 3H, $C\underline{H}_3$); 2.20 (s, 3H, $C\underline{H}_3$). ^{13}C NMR(400 MHz, $CDCl_3$, TMS, 25 °C): δ (ppm) = 142.6 (N<u>C</u>HN,C_1). 138.9 (C_{14}); 137.2 (C_6); 137.1 (C_4); 135.5 ($C_{19,25}$); 130.3 (C_2); 130.2 (C_9); 129.9 (2<u>C</u>H,$C_{12,17}$); 129.8 (C_{11}); 129.4 (4<u>C</u>H, $C_{21,23,27,29}$); 129.3 (2<u>C</u>H, $C_{22,28}$); 128.4 (4<u>C</u>H, $C_{20,24,26,30}$); 128.1 (2<u>C</u>H, $C_{13,16}$); 114.5 (<u>C</u>H, C_3); 113.4 (<u>C</u>H, C_8); 66.4 (<u>C</u>H, C_{18}); 51.2 (N-<u>C</u>H_2, C_{10}); 21.1 (<u>C</u>H_3, C_{15}); 20.7 (<u>C</u>H_3, C_7); 20.6 (<u>C</u>H_3, C_5). Elemental analysis calcd. (%) for $C_{30}H_{29}ClN_2$ (M.w. = 453.02 g/mol): C 79.54, H 6.45, N 6.18; found (%): C 79.28, H 6.73, N 5.35

1-Benzhydryl −5,6-dimethyl-3-(2,4,6-trimethylbenzyl)benzimidazolium chloride (2c)

Yield 81% (390 mg, white solid); m.p = 155–156 °C; FT-IR $\nu_{(CN)}$ = 1546 cm^{-1}. ^{1}H NMR (400 MHz, $CDCl_3$, TMS, 25 °C): δ (ppm) = 10.88 (s, 1H, NC<u>H</u>N), 7.50 (s, 1H, N-$C_6\underline{H}_2(CH_3)_2$-N), 7.36 (dd, *J* = 5.3 Hz, 1.6 Hz, 6H, C<u>H</u>-Ar); 7.31 (dd, *J* = 7.0 Hz, 2.5 Hz, 4H,C<u>H</u>-Ar); 6.94 (s, 1H, CH-Ar); 6.92 (s, 1H, Ph-C<u>H</u>-Ph); 6.86 (s, 2H, C<u>H</u>-Ar); 5.88 (s, 2H, $C\underline{H}_2$N); 2.26 (s, 6H, $C\underline{H}_3$); 2.24 (s, 3H, $C\underline{H}_3$); 2.20 (s, 3H, $C\underline{H}_3$); 2.17 (s, 3H, $C\underline{H}_3$). ^{13}C NMR (400 MHz, $CDCl_3$, TMS, 25 °C): δ (ppm) = 142.8 (N<u>C</u>HN,C_1); 139.4 (C_{15}); 137.8 ($C_{12,18}$); 137.0 (C_4); 136.9 (C_6); 135.6 ($C_{21,27}$); 130.4 (C_2); 130.0 (2<u>C</u>H, $C_{14,17}$); 129.9 (C_9); 129.3 (4CH $C_{23,25,29,31}$); 129.2 (2<u>C</u>H, $C_{24,30}$); 128.3 (4<u>C</u>H, $C_{22,26,28,32}$); 125.5 (C_{11}); 114.5 (<u>C</u>H, C_3); 113.6 (<u>C</u>H, C_8); 66.2 (<u>C</u>H, C_{20}); 47.4 (N-<u>C</u>H_2, C_{10}); 21.0 (<u>C</u>H_3, C_{16}); 20.7 (<u>C</u>H_3, C_7); 20.6 (<u>C</u>H_3, C_5); 20.2 (2<u>C</u>H_3, $C_{13,19}$). Elemental analysis calcd. (%) for $C_{32}H_{33}ClN_2$ (M.w. = 481.08 g/mol): C 79.89, H 6.91, N 5.82; found (%): C 79.71, H 6.86, N 6.38

1-Benzhydryl −5,6-dimethyl-(2-methylbenzyl)benzimidazolium chloride (2d)

Yield 82% (372 mg, white solid); m.p = 151–152 °C; FT-IR $\nu_{(CN)}$ = 1541 cm^{-1}. ^{1}H NMR (400 MHz, $CDCl_3$, TMS, 25 °C): δ (ppm) = 11.06 (s, 1H, NC<u>H</u>N), 7.39–7.33 (m, 11*H*, C<u>H</u>-Ar), 7.33 (s, 1H, C<u>H</u>-Ar); 7.21–7.13 (m, 3H, C_6H_4); 7.08 (d, *J* = 7.2 Hz, 1H, C<u>H</u>-Ar); 6.98 (s, 1H, Ph-C<u>H</u>-Ph); 5.92 (s, 1H, $C\underline{H}_2$N); 2.27 (s, 6H, $C\underline{H}_3$); 2.20 (s, 3H, $C\underline{H}_3$). ^{13}C NMR (400

MHz, $CDCl_3$, TMS, 25 °C): δ (ppm) = 142.5 (NCHN,C_1); 139.1 (C_{12}); 137.3 (C_4); 137.1 (C_6); 135.5 ($C_{19,25}$); 133.1 (C_{11}); 130.3 (C_2); 129.8 (C_9); 129,7 (CH, C_{17}); 129.4 (4CH, $C_{21,23,27,29}$); 129.3 (2CH, $C_{22,28}$); 129.1 (CH, C_{15}); 128.5 (CH, C_{16}); 128.4 (4CH, $C_{20,24,26,30}$); 125.0 (C_{14}); 114.4 (CH, C_3); 113.4 (CH, C_8); 66.4 (CH, C_{18}); 51.3 (N-CH_2, C_{10}); 21.3 (CH_3, C_{13}); 20.7 (CH_3, C_7); 20.6 (CH_3, C_5). Elemental analysis calcd. (%) for $C_{30}H_{29}ClN_2$ (M.w. = 453.02 g/mol): C 79.54, H 6.45, N 6.18; found (%): C 79.74, H 6.36, N 6.13

1-Benzhydryl −5,6-dimethyl-(4-tert-butylbenzyl)benzimidazolium bromide (2e)

Yield 71% (384 mg, white solid); m.p = 179–180 °C; FT-IR $\nu_{(CN)}$ = 1542 cm^{-1}. ^1H NMR (400 MHz, $CDCl_3$, TMS, 25 °C): δ (ppm) = 10.73 (s, 1H, NCHN), 7.42–7.37 (m, 11*H*, CH-Ar); 7.34 (sl, 5H, CH); 7.00 (s, 1H, Ph-CH-Ph); 5.84 (s, 2H, CH_2N); 2.31 (s, 3H, CH_3); 2.22 (s, 3H, CH_3); 1.25 (s, 9H, CH_3). ^{13}C NMR (400 MHz, $CDCl_3$, TMS, 25 °C): δ (ppm) = 152.1 (C_{14}); 141.6 (NCHN,C_1); 137.3 (C_4); 137.2 (C_6); 135.3 ($C_{22,28}$); 130.4 (C_{11}); 129.9 (C_2); 129.8 (C_9); 129.4 (4CH, $C_{24,26,30,32}$); 129.3 (2CH, $C_{25,31}$); 128.4 (4CH, $C_{23,27,29,33}$); 127.8 (2CH, $C_{12,20}$); 126.2 (2CH, $C_{13,19}$); 114.4 (CH, C_3); 113.4 (CH, C_8); 66.4 (CH, C_{21}); 51.1 (N-CH_2, C_{10}); 34.6 (C_{15}); 31.1 (3CH_3, $C_{16,17,18}$); 20.7 (CH_3, C_7); 20.6 (CH_3, C_5). Elemental analysis calcd. (%) for $C_{33}H_{35}BrN_2$ (M.w. = 539.56 g/mol): C 73.46, H 6.54, N 5.19; found (%):C 73.15, H 6.28, N 5.20

1-Benzhydryl-5,6-dimethyl-3-(3,4,5-trimethoxybenzyl)benzimidazolium bromide (2f)

Yield 70% (373 mg, white solid); m.p = 157–158 °C; FT-IR $\nu_{(CN)}$ = 1552 cm^{-1}. ^1H NMR (400 MHz, $CDCl_3$, TMS, 25 °C): δ (ppm) = 11.25 (s, 1H, NCHN); 7.42–7.32 (m, 12H, CH-Ar), 6.98 (s, 1H, Ph-CH-Ph); 6.76 (s, 2H, C_6H_2), 5.81 (s, 2H, CH_2N); 3.79 (s, 6H, OCH_3); 3.78 (s, 6H, OCH_3); 2.33 (s, 3H, CH_3); 2.23 (s, 3H, CH_3). ^{13}C NMR (400 MHz, $CDCl_3$, TMS, 25 °C): δ (ppm) = 153.72 ($C_{13,17}$); 142.70 (NCHN, C_1); 138.38 (C_{15}); 137.30 (C_4); 137.21 (C_6); 135.50 ($C_{21,27}$); 130.28 (C_2); 129.77 (C_2); 128.78 (C_{11}); 129.41 (4CH, $C_{23,25,29,31}$); 129.38 (2CH, $C_{24,30}$); 128.40 (4CH, $C_{22,26,28,32}$); 114.41 (CH, C_3); 113.4 (CH, C_8); 105.69 (2CH, $C_{12,19}$); 66.46 (CH, C_{20}); 60.84 (OCH_3, C_{16}); 56.53 (2OCH_3, $C_{14,18}$); 51.43 (N-CH_2, C_{10}); 20.8 (2CH_3, $C_{5,7}$). Elemental analysis calcd. (%) for $C_{32}H_{33}ClN_2O_3$ (M.w. = 529.07 g/mol): C 72.65, H 6.29, N 5.29; found (%): C 72.47, H 6.51, N 5.32

2.1.3. General procedure for preparation of Ag(I)–NHC complexes (3a-f)

The complexes of silver(I)–NHC were prepared with the method of Organ [20]. According to the use of benzimidazolium salts (1 mmol) with Ag_2O (1.5 mmol) in dry chloroform at 50 °C for 48 h, in dark conditions, under argon and covered with aluminum foil. The reaction mixture was filtered through celite, and the solvent was removed under vacuum to afford the product. The salts were converted to silver(I)–NHC complexes automatically by the reaction, which allowed us to obtain a solution mixture, that affords a white solid as silver(I)–NHC. The resulting white solid was isolated by filtration then dried in a vacuum, and recrystallized in $CHCl_3/Et_2O$.

μ-Dikloro-bis-{[1-benzhydryl-3-(2,3,5,6-tetramethylbenzyl)-5,6-dimethylbenzimidazole-2-ylidene]silver(I) (3a). Yield 70% (0.422 g, white solid); m.p = 245–246 °C; FT-IR $\nu_{(CN)}$ = 1542 cm^{-1}. ^1H NMR (400 MHz, $CDCl_3$, TMS, 25 °C): δ (ppm) = 7.37–7.32 (m, 7H, CH); 7.21 (s, 1H, C_6H_1); 7.17 (dd, *J* = 6.1 Hz, 2.6 Hz, 4H, CH-Ar); 7.10 (s, 2H, N-$C_6H_2(CH_3)_2$-N); 6.81 (s, 1H, Ph-CH-Ph); 5.49 (s, 2H, CH_2N); 2.29 (s, 3H, CH_3); 2.28 (s, 6H, CH_3); 2.19 (s, 3H, CH_3); 2.14 (s, 6H, CH_3). ^{13}C NMR (400 MHz, $CDCl_3$, TMS, 25 °C): δ (ppm) = 137.4 (CH, $C_{22,28}$); 135.1 ($C_{14,17}$); 133.5 ($C_{12,19}$); 133.4 (C_4); 133.4 (C_6); 133.0 (C_{11}); 129.9 (CH, C_{16}); 128.9 (4CH, $C_{24,26,30,32}$); 128.5 (2CH, $C_{25,31}$); 128.31(4CH, $C_{23,27,29,33}$); 113.6 (CH, C_3); 111.7 (CH, C_8); 68.6 (CH, C_{21}); 48.1 (CH_2, C_{10}); 20.7 (2CH_3,$C_{15,18}$); 20.4 (CH_3, C_7); 20.4 (CH_3,C_5); 16.2 (2CH_3, $C_{13,20}$). Elemental analysis calcd. (%) for $C_{64}H_{68}Ag_2Cl_2N_4$ (M.w. = 1179.90 g/mol): C 65.15, H 5.81, N 4.75; found (%): C 66.04, H 5.95, N 4.51

Chloro[1-benzhydryl-3-(4-methylbenzyl)-5,6-dimethylbenzimidazole-2-ylidene]silver(I) (3b). Yield 80% (0.450 g, white solid); m.p = 144–145 °C; FT-IR $\nu_{(CN)}$ = 1542 cm^{-1}. ^1H NMR (400 MHz, $CDCl_3$, TMS, 25 °C): δ (ppm) = 7.39 (m, 7H, CH-Ar); 7.22 (m, 4H, CH-Ar); 7.14 (s, 1H, N-$C_6H_2(CH_3)_2$-N); 7.12 (sl, 4H, C_6H_4); 7.09 (s, 1H, N-$C_6H_2(CH_3)_2$-N); 6.92 (s, 1H, Ph-CH-Ph); 5.52 (s, 2H, CH_2N); 2.31 (s, 3H, CH_3); 2.26 (s, 3H, CH_3); 2.20 (s, 3H, CH_3). ^{13}C NMR (400 MHz, $CDCl_3$, TMS, 25 °C): δ (ppm) = 138.2 (C_{14}); 137.3 ($C_{19,25}$); 133.9 (C_6); 133.6 (C_4); 132.9 (C_2); 132.5 (C_9); 132.0 (C_{11}); 129.7 (2CH, $C_{13,15}$); 129.2 (4CH, $C_{21,23,27,29}$); 128.7 (2CH, $C_{22,28}$); 128.3 (4CH, $C_{20,24,26,30}$); 126.9 (2CH, $C_{12,17}$); 112.9 (CH, C_3); 112.3 (CH, C_8); 66.9 (CH, C_{18}); 53.8 (CH_2, C_{10}); 21.1 (CH_3, C_{15}); 20.4 (CH_3, C_7); 20.3 (CH_3, C_5). Elemental analysis calcd. (%) for $C_{30}H_{28}AgClN_2$ (M.w. = 559.88 g/mol): C 64.36, H 5.04, N 5.00; found (%): C 64.64, H 5.19, N 5.12

Chloro[1-benzhydryl-3-(2,4,6-trimethylbenzyl)-5,6-dimethylbenzimidazole-2-ylidene]silver(I) (3c). Yield 74% (0.435 g, white solid); m.p = 200–201 °C; FT-IR $\nu_{(CN)}$ = 1542 cm^{-1}. ^1H NMR (400 MHz, $CDCl_3$, TMS, 25 °C): δ (ppm) = 7.36 (m, 7H, CH); 7.19 (m, 5H, CH); 6.94 (s, 2H, C_6H_2); 6.92 (s, 1H, N-$C_6H_2(CH_3)_2$-N); 6.84 (s, 1H, Ph-CH-Ph); 5.51 (s, 2H, CH_2N); 2.32 (s, 3H, CH_3); 2.23 (s, 9H, CH_3); 2.18 (s, 3H, CH_3). ^{13}C NMR (400 MHz, $CDCl_3$, TMS, 25 °C): δ (ppm) = 139.2 (C_{15}); 137.4 ($C_{21,27}$); 137.4 ($C_{12,18}$); 133.5 (C_6); 133.4 (C_4); 130.1 ($C_{14,17}$); 129.0 (4CH, $C_{23,25,29,31}$); 128.6 (2CH, $C_{24,30}$); 128.3 (4CH, $C_{22,26,28,32}$); 126.9 (C_{11}); 113.3 (CH, C_3); 112.0 (CH, C_8); 68.0 (CH, C_{20}); 48.7 (N-CH_2, C_{10}); 21.1 (CH_3, C_{16}); 20.5 (2CH_3, $C_{13,19}$); 20.4 (CH_3, C_7); 20.4 (CH_3, C_5). Elemental analysis calcd. (%) for $C_{32}H_{32}AgClN_2$ (M.w. = 559.88 g/mol): C 64.37, H 5.49, N 4.76; found (%): C 64.74, H 5.65, N 4.78

Chloro[1-benzhydryl-3-(2-methylbenzyl)-5,6-dimethylbenzimidazole-2-ylidene]silver(I) (3d). Yield 90% (0.532 g, white solid); m.p = 222–223 °C; FT-IR $\nu_{(CN)}$ = 1542 cm^{-1}. ^1H NMR (400 MHz, $CDCl_3$, TMS, 25 °C) : δ (ppm) = 7.39 (s, 7H, CH-Ar); 7.23 (m, 4H, CH-Ar); 7.20 (s, 1H, CH-Ar); 7.16 (s, 1H, N-$C_6H_2(CH_3)_2$-N); 7.10 (s, 1H, CH-Ar); 7.08 (s, 1H, CH-Ar); 7.00 (m, 2H, CH-Ar);0.6.94 (s, 1H, Ph-CH-Ph); 5.53 (s, 2H, CH_2N); 2.31 (s, 3H, CH_3); 2.26 (s, 3H, CH_3); 2.21 (s, 3H, CH_3). ^{13}C NMR (400 MHz, $CDCl_3$, TMS, 25 °C): δ (ppm) = 138.8 (C_{12}); 137.3 ($C_{19,25}$); 134.9 (C_{11}); 133.9 (CH, C_4); 133.3 (CH, C_6); 132.9 (CH, C_2); 132.5 (CH, C_9); 129.2 (4CH, $C_{21,23,27,29}$); 129.1 (CH, C_{15}); 128.9 (CH, C_{16}); 128.8 (2CH, $C_{22,28}$); 128.3 (4CH, $C_{20,24,26,30}$); 123.9 (C_{17}); 112.9 (CH, C_3); 112.2 (CH, C_8); 66.9 (CH, C_{18}); 53.9 (N-CH_2, C_{10}); 21.4 (CH_3, C_{13}); 20.4 (CH_3, C_7); 20.3 (CH_3, C_5). Elemental analysis calcd. (%) for $C_{32}H_{32}AgClN_2$ (M.w. = 559.88 g/mol): C 64.36, H 5.04, N 5.00; found (%): C 64.96, H 5.31, N 4.95.

Bromo[1-benzhydryl-3-(4-tert-butylbenzyl)-5,6-dimethylbenzimidazole-2-ylidene]silver(I) (3e). Yield 70% (0.433 g, white solid); m.p = 219–220 °C; FT-IR $\nu_{(CN)}$ = 1542 cm^{-1}. ^1H NMR (400 MHz, $CDCl_3$, TMS, 25 °C): δ (ppm) = 7.39 (m, 7H, CH-Ar); 7.34 (s, 1H, CH-Ar); 7.32 (s, 1H, C_6H_4); 7.22 (m, 4H, CH-Ar); 7.17 (s, 1H, N-$C_6H_2(CH_3)_2$-N); 7.15 (s, 2H, C_6H_4); 7.12 (s, 1H, N-$C_6H_2(CH_3)_2$-N); 6.93 (s, 1H, Ph-CH-Ph); 5.54 (s, 2H, CH_2N); 2.27 (s, 3H, CH_3); 2.21 (s, 3H, CH_3); 1.28 (s, 9H, CH_3 (*t*-Bu)). ^{13}C NMR (400 MHz, $CDCl_3$, TMS, 25 °C): δ (ppm) = 151.3 (C_{14}); 137.3 ($C_{22,28}$); 133.9 (C_4); 133.5 (C_6); 132.9 (C_9); 132.6 (C_2); 132.0 (C_{11}); 129.4 (C); 129.2 (4CH, $C_{24,26,30,32}$); 128.7 (2CH, $C_{25,31}$); 128.4 (C); 128.3 (4CH, $C_{23,27,29,33}$); 126.6 (2CH, $C_{13,19}$); 125.9 (2CH, $C_{12,20}$); 114.4 (CH, C_3); 113.5 (CH, C_8); 66.9 (CH, C_{21}); 53.6 (N-CH_2, C_{10}); 34.5 (C_{15}); 31.2 (3CH_3, $C_{16,17,18}$); 20.4 (CH_3, C_7); 20.3 (CH_3, C_5). Elemental analysis calcd. (%) for $C_{33}H_{34}AgClN_2$ (M.w. = 601.96 g/mol): C 65.84, H 5.69, N 4.65; found (%): C 65.94, H 5.92, N 4.43.

Chloro[1-benzhydryl-3-(3,4,5-trimethoxybenzyl)-5,6-dimethylbenzimidazole-2-ylidene] silver(I) (3f). Yield 80% (0.540 g, white solid); m.p = 117–118 °C; FT-IR $\nu_{(CN)}$ = 1542 cm^{-1}. ^1H NMR (400 MHz, $CDCl_3$, TMS, 25 °C): δ (ppm) = 7.38 (m, 7H, CH-Ar); 7.22 (m, 4H, CH-Ar); 7.15 (s, 1H,

Table 1
Crystal data and structure refinement parameters for **2c**, **2f,** and **3a**.

Parameters	3,5-dimethylbenzimidazolium salts		Silver(I)–NHC complex
	2c	**2f**	**3a**
CCDC depository	2,058,369	2,058,370	2,058,371
Color/shape	Colorless/ prism	Colorless/plate	Colorless/plate
Chemical formula	$(C_{32}H_{33}N_2)^+$ Cl^- $2H_2O$	$(C_{32}H_{33}N_2O_3)^+$ $Cl^-CH_2Cl_2$	$[Ag_2Cl_2(C_{33}H_{34}N_2)_2]$
Formula weight	517.08	613.98	1203.88
Temperature (K)	296(2)	296(2)	296(2)
Wavelength (Å)	0.71073 Mo Kα	0.71073 Mo Kα	0.71073 Mo Kα
Crystal system	Monoclinic	Triclinic	Monoclinic
Space group	$P2_1/c$ (No. 14)	P (No. 2)	$C2/c$ (No. 15)
Unit cell parameters			
a, b, c (Å)	13.5311(12), 16.4277(17), 14.5904(13)	10.9830(8), 12.0714 (8),12.0148(9)	27.6791(19), 9.3376 (7), 22.9241(16)
α, β, γ (°)	90, 116.407 (6), 90	85.937(6), 86.665(6), 85.163(6)	90, 106.436(5), 90
Volume ($Å^3$)	2904.8(5)	1581.1(2)	5682.8(7)
Z	4	2	4
$D_{calc.}$ (g/cm^3)	1.182	1.290	1.407
μ (mm^{-1})	0.162	0.325	0.827
Absorption correction	Integration	Integration	Integration
$T_{min.}$, $T_{max.}$	0.9231, 0.9490	0.9128, 0.9867	0.7750, 0.9776
F_{000}	1104	644	2480
Crystal size (mm^3)	0.62 × 0.37 × 0.36	0.49 × 0.19 × 0.06	0.55 × 0.21 × 0.02
Diffractometer/ measurement method	STOE IPDS II/ ω scans	STOE IPDS II/ω scans	STOE IPDS II/ω scans
Index ranges	$-16 \le h \le 16$, $-19 \le k \le 18$, $-16 \le l \le 16$	$-13 \le h \le 12$, $-14 \le k \le 12$, $-14 \le l \le 14$	$-32 \le h \le 32$, $-11 \le k \le 11$, $-27 \le l \le 27$
θ range for data collection (°)	$1.680 \le \theta \le 25.047$	$2.322 \le \theta \le 25.047$	$1.534 \le \theta \le 25.049$
Reflections collected	15,167	14,288	24,599
Independent/ observed reflections	4965/1707	5581/2845	5037/2296
$R_{int.}$	0.1204	0.0781	0.1441
Refinement method	Full-matrix least-squares on F^2	Full-matrix least-squares on F^2	Full-matrix least-squares on F^2
Data/restraints/ parameters	4965/0/339	5581/0/378	5037/0/339
Goodness-of-fit on F^2	0.945	1.030	0.984
Final R indices [$I > 2\sigma(I)$]	$R_1 = 0.1148$, $wR_2 = 0.2957$	$R_1 = 0.0734$, $wR_2 = 0.1244$	$R_1 = 0.0764$, $wR_2 = 0.1382$
R indices (all data)	$R_1 = 0.2210$, $wR_2 = 0.3492$	$R_1 = 0.1565$, $wR_2 = 0.1492$	$R_1 = 0.1820$, $wR_2 = 0.1739$
$\Delta\rho_{max.}$, $\Delta\rho_{min.}$ ($e/Å^3$)	0.36, −0.31	0.18, −0.28	0.61, −0.48

N-$C_6\underline{H}_2$-$(CH_3)_2$-N); 7.14 (s, 1H, N-$C_6\underline{H}_2$-$(CH_3)_2$-N); 6.96 (s, 1H, Ph-C<u>H</u>-Ph); 6.43 (S, 2H, C<u>H</u>-Ar), 5.50 (s, 2H, $C\underline{H}_2$N); 3.82 (s, 3H, $OC\underline{H}_3$); 3.77 (s, 6H, $OC\underline{H}_3$); 2.30 (s, 3H, $C\underline{H}_3$); 2.23 (s, 3H, $C\underline{H}_3$). ^{13}C NMR (400 MHz, $CDCl_3$, TMS, 25 °C): δ (ppm) = 153.6 ($C_{13,17}$); 137.9 (C_{15}); 137.3 ($C_{21,27}$); 134.1 (C_4); 133. (C_6); 130.7 (C_{11}); 129.4 (C_9); 129.2 (4<u>C</u>H, $C_{23,25,29,31}$); 128.8 (2<u>C</u>H, $C_{24,30}$); 128.4 (C_2); 128.3 (4<u>C</u>H, $C_{22,26,28,32}$); 112.9 (<u>C</u>H, C_3); 112.1 (<u>C</u>H, C_8); 105.7 (2CH, $C_{12,19}$); 66.8 (<u>C</u>H, C_{20}); 60.9 ($OC\underline{H}_3$, C_{16}); 56.2 (2$OC\underline{H}_3$, $C_{14,18}$); 53.8 (N-$C\underline{H}_2$, C_{10}); 20.4 ($C\underline{H}_3$, C_7); 20.4 ($C\underline{H}_3$, C_5). Elemental analysis calcd. (%) for $C_{32}H_{33}AgClN_2O_3$ (M. w. = 635.12 g/mol): C 60.44, H 5.07, N 4.41; found (%): C 60.33, H 5.59, N 3.96.

2.2. X-Ray crystallographic analysis study

The structure of 3,5-dimethylbenzimidazolium salts **2c**, **2f**, and Ag-NHC complex **3a** was determined by the X-ray diffraction technique, the obtained results confirmed all the spectroscopic data. A suitable single crystal of complex **2c**, **2f**, and **3a** for X-ray diffraction analysis was were grown by slow diffusion of diethyl ether in a saturated chloroform solution at room temperature. Crystallographic data of **2c**, **2f**, and **3a** were gathered with an STOE IPDS II diffractometer using graphite-monochromated Mo Kα radiation by applying the ω -scan method at room temperature. X-AREA was used for data collection and cell refinement. [21] while data reduction was applied using X-RED32 [21]. The structures were solved using the charge-flipping algorithm by SUPERFLIP [22] and refined using the full-matrix least-squares calculations on F^2 using SHELXL-2018 [23]. The H atoms were calculated geometrically and a riding model was applied during the refinement process. Crystal data, data collection, and structure refinement details are collected in Table 1. Molecular graphics were generated by using OLEX2 [24].

2.3. Biological capacity study

All the synthesized 3.5-dimethylbenzimidazolium salts **2a-f** and their related silver(I)–NHC complexes **3a-f** were tested for antimicrobial, Anti-Cholinesterase **(**anti-Alzheimer**),** anti-Lipase, and anti-Alpha-amylase (anti-Diabetic**)** activities.

2.3.1. Material

Candida albicans (ATCC MYA-2876) and *Candida glabrata* (ATCC 2001), which are pathogenic yeast species, were used in antifungal tests, and *Escherichia coli* (ATCC 25922), *Staphylococcus aureus* (ATCC 29213), and *Pseudomonas aeruginosa* (ATCC 27853) species were used antibacterial tests. All types of bacteria and fungi used in the study were provided by the Molecular Genetics Laboratory of the Department of Genetics at İnönü University Turgut Özal Medical Faculty (Battalgazi, Malatya, Turkey).

The acetylthiocholine iodide, butyrylthiocholine chloride which was employed as substrates of the reaction were obtained from Sigma Chemical Co (Sigma-Aldrich GmbH, Stern-Heim, Germany). The AChE from Electrophorus electricus eel-AChE (Type-VI-S, EC 3.1.1.7, 425.84 U/mg) and horse serum butyrylcholinesterase eq BChE, (EC 3.1.1.8, 11.4 U/mg), which are enzymes that were used in anticholinesterase assay, were obtained from Sigma-Aldrich. All other chemicals and solvents were of analytical grade. The measurements and calculations of the enzymatic activity results were evaluated by using quantitative colorimetric assay, they were carried out on a 96-well microplate reader, (PerkinElmer Multimode Plate Reader EnSpire, USA) at the Center of Biotechnology Research. (Ali Mendjli, Constantine, Algeria)

2.3.2. Methods

2.3.2.1. Antibacterial activity

2.3.2.1.1. Determination of the minimum inhibitory concentration (MIC). Antifungal and antibacterial MIC (Minimal Inhibitory Concentration) analysis was performed using the BMD (Broth Microdilution) test, as described in EUCAST EDef 7.3.2 [25] for yeasts and CLSI M07-A10 [26] for bacteria. Briefly, the broth micro-dilution technique using a 96-wells microplate was used to determine the minimum inhibitory concentration (MIC) (Erdemoglu et al., 2007). The selected compounds (NHCs) were dissolved in dimethylsulfoxide (DMSO), and serial dilutions were made in a flat-bottom sterile 96-well microplate, in SDB (Sabouraud Dextrose Broth) medium (1% peptone, 2% glucose, pH 5.6) [27] for yeasts, and LB (Luria-Bertani) broth medium (1% tryptone, 1% NaCl, 0.5% yeast extract, pH 7.0) [28] for bacteria. In sterile water, yeast (1-5x10^5 CFU/mL) and bacteria (1x10^6 CFU/mL) cell solutions

(inoculums) were prepared and added in equal volumes to wells containing different concentrations of the compounds. After the cell solutions were added, the compounds' final concentrations were between 0.8 and 800 mg/L, and the cell concentrations were 0.5–2.5x10^5 CFU/mL for yeasts and 5x10^5 CFU/mL for bacteria in the final step. Finally, the microplate was covered and incubated at 37 °C for 24 h for yeasts and 16–18 h at 37 °C for bacteria. The MIC was determined spectrophotometrically at 530 nm after incubation in yeasts and by naked eyes in bacteria. The MIC value was measured as the lowest drug concentration causing at least 50% or more reduction in yeasts' growth compared to the control (no drug) cell group, and as the lowest drug concentration without visible growth in bacteria. Ampicillin, Tetracycline, Amphotericin B, and Voriconazole were used as the reference drugs.

2.3.2.2. Enzymatic evaluation. This study evaluated the capacity of the novel benzimidazolium salts and silver (I)–NHC complexes as inhibitors of different enzymes. In this context, all compounds were evaluated against a panel of important biological activities such as anticholinesterase, anti-Lipase, and anti-diabetic activities.

a. Anti-Cholinesterase assay (Anti-Alzheimer)

Cholinesterase family inhibitors of acetylcholinesterase (AChE) and butyrylcholinesterase (BChE) are the most investigated and common strategy used for the treatment of Alzheimer's disease [29–32]. Acetylcholinesterase (AChE) and butyrylcholinesterase (BChE) inhibitory activities of the new compound were done according to the method described by Rhee et *al.* [33]. based on the spectrophotometric method of Ellman's [34] with slight modifications. In this experiment, a reaction volume of 200 μL consisting, 150 μL of sodium phosphate buffer (100 mM, Ph = 8.0), 10 μL of the sample at different concentrations in methanol, and 20 μL of AChE or BChE solution in buffer was mixed and left to incubate for 15 min at 37 °C, Afterwards, 10 μL of DTNB (0.5 mM) were added. After that, 10 μL of acetylthiocholine iodide or 10 μL of butyrylthiocholine chloride (0.2 mM). was added to start the reaction. The hydrolysis of these substrates was monitored spectrophotometrically by the formation of yellow 5-thio-2-nitrobenzoate anion as the result of the reaction of DTNB with thiocholine released by the enzymatic hydrolysis of acetylthiocholine iodide or butyrylthiocholine chloride. The absorbance of the solution was measured at 412 nm by the use of a 96-well microplate reader (Perkin Elmer, Enspire). The results were given as IC_{50} values (μM) corresponding to the 50% inhibition concentration. Percentage of inhibition I (%) was determined using the following formula

$$\text{Inhibition (I \%)} = (\text{E} - \text{S} / \text{S}) \times 100$$

Where E is the activity of the enzyme without a test sample, and S is the activity of the enzyme in the presence of the test sample. The measurements were carried out in triplicate and Galanthamine was used as a reference compound.

b. Anti-lipase assay

The assay to determine the inhibitory capacity against pancreatic lipase was performed according to the method of (Souza, 2009) [35] with minor modification. Briefly, in this experiment the selected compounds were prepared at the concentration of 4 mM in dimethyl sulfoxide (DMSO). A reaction volume of 200 μL in triplicate consisting, 50 μL of a sample at different concentrations in DMSO with 100 μL of pancreatic Lipase solution in Tris-HCl buffer (pH = 8) were mixed and incubated for 20 min at 37 °C, Afterwards, The reaction was then initiated by the addition of 50 μL of *p*-Nitrophenol Palmitate (*p*-NPP) after incubation for 2 h at 37 °C. A blank with DMSO instead of enzyme solution was prepared. orlistat was used as a positive control. The absorbances of lipase products (*p*-nitrophenol) were measured using a 96-well microplate reader (Perkin Elmer, Enspire) at 410 nm. The findings were expressed as IC_{50} values. (μM) corresponding to the 50% inhibition concentration. The percent inhibition I (%) of pancreatic lipase was determined using the following equation [36].

$$\text{I}(\%) = [(\text{A} - \text{a}) - (\text{B} - \text{b})/(\text{A} - \text{a})] \times 100$$

Where **A**: is the absorbance in the absence of the possible inhibitor, which corresponds to the control enzyme assay; **a**: is the absorbance in the absence of the sample and enzyme (blank substrate); **B**: is the absorbance in the presence of the possible inhibitor with the enzyme and substrate; **b**: is the absorbance in the absence of the enzyme.

c. Anti-α-amylase activity

The inhibitory activity of alpha-amylase was tested using the iodine /potassium iodide (IKI) method according to (G. Zengin et al. 2014) [37]. With some modifications. Briefly, in this experiment, the assay was conducted by mixing of 25 μL of the sample at different concentrations in methanol with 50 μL of α amylase solution in 1U of sodium phosphate buffer (*p*H = 6.9 with 6 Mm NaCl) and incubated for 10 min at 37 °C, Afterwards, 50 μL of Amidon (0.1%), was added. Similarly, by adding sample solution to all reaction reagents, a blank was prepared without enzyme (α-amylase) solution. For 20 min, the reaction mixture was incubated at 37 °C. After incubation, The reaction was then stopped by the addition of HCl 25 μL (1 M), finally, the reaction was initiated by the addition of 100 μL of (IKI) iodine-potassium iodide solution. The absorbance of the solution was measured at 630 nm by the use of a 96-well microplate reader (Perkin Elmer, Enspire). The results were presented as IC_{50} values (μM) corresponding to 50% inhibition concentration. The acarbose was used as a reference. The percentage of inhibition I (%) was calculated as follows in the formula:

$$\boldsymbol{I}\ \% = \mathbf{1} - [(\text{Ac} - \text{Ae}) - (\text{As} - \text{Ab})/(\text{Ac} - \text{Ae})]$$

As = Absorbance [Extrait, Enzyme, Amidon, HCl, IKI]; $\mathbf{A_b}$ = Absorbance [Extrait, sodium phosphate buffer, IKI]; $\mathbf{A_e}$ = Absorbance [solvant vol Extrait, Enzyme, Amidon, HCl, IKI]; $\mathbf{A_c}$ = Absorbance [solvant vol Extrait, sodium phosphate buffer, Amidon, HCl, IKI]

2.4. Statistical analysis

All data on activity tests were the averages of triplicate analyses. The data were recorded as means ± standard error meaning. Significant differences between means were determined by Student's *t*-test; p values < 0.05 were regarded as significant.

2.5. Molecular docking study

Molecular modeling studies were accomplished to investigate the possible binding mode of the designed compounds into BChE and AChE active sites. Before docking, the crystal structures of human AChE (PDB ID: 4M0E [38]) and BChE (PDB ID: 2XQF [39]) were downloaded from the Protein Data Bank. The binding site of these enzymes was defined by selecting all the residues with at least one heavy atom within 6 Å from the inhibitor of the crystal structure. This selection was refined by adding every residue beyond 6 Å considered essential for the continuity of the cavity [40]. Then, AChE and BChE were prepared using the Protein Preparation Wizard of Schrodinger [41] by removing their Chain B, water molecules, heteroatoms, and co-factors. Hydrogen and missing atoms were added and bond charges were computed. Finally, the intramolecular energy was minimized and a mol2 file was exported and used as a starting structure for docking [42]. Meanwhile, the synthesized compounds were drawn and prepared using the built and LigPrep module implemented in Maestro version 11.3 of the Schrodinger suite [43]. This preparation was carried out in order to create several structures for each molecule. (up to 32) with different enantiomers (when

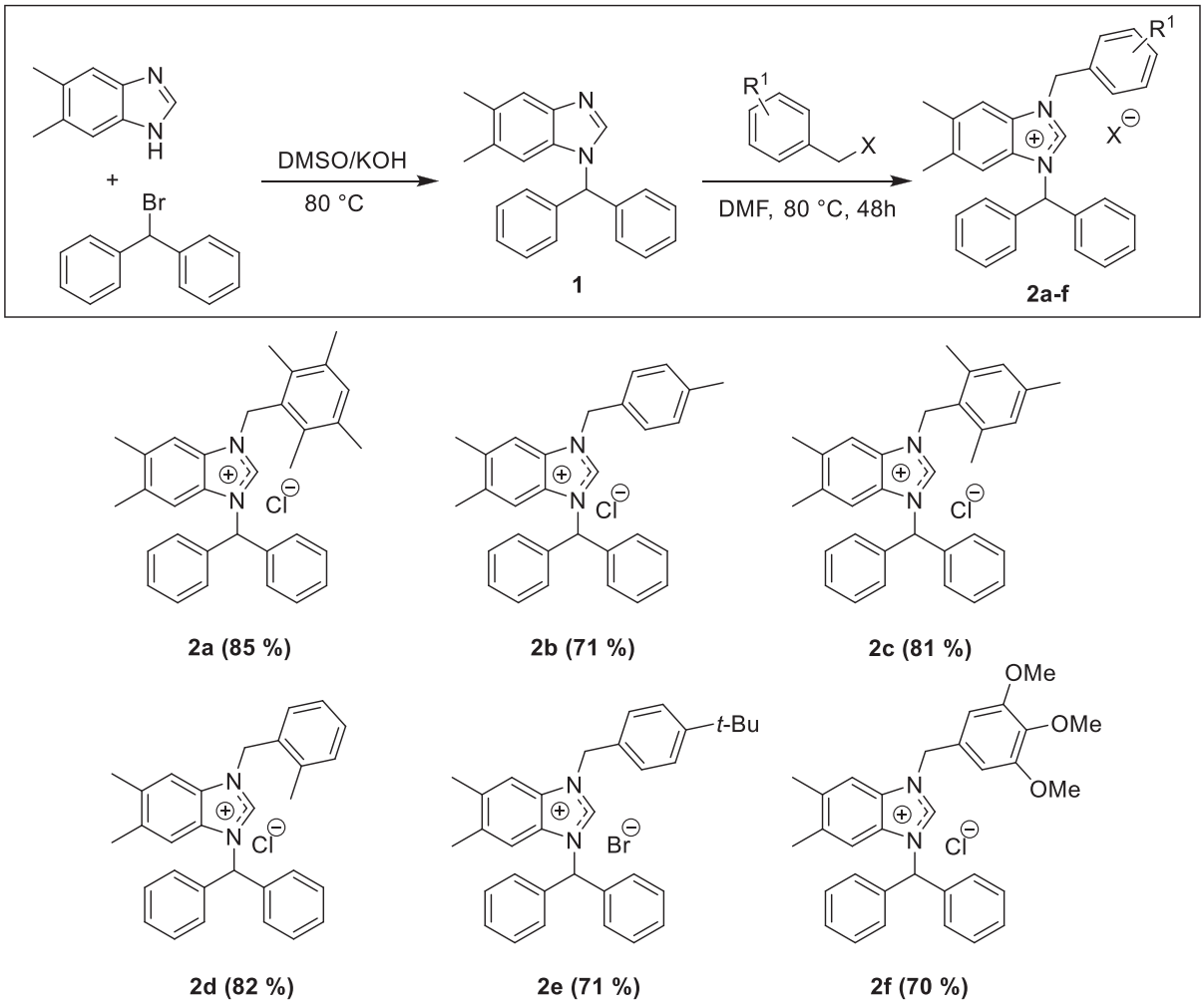

Scheme 1. Synthetic route for the preparation of benzimidazolium salts **2a-f.**

undefined), protonation states at pH = 7.4 ± 1, and tautomers [44]. All the conformations generated were minimized and exported as mol2 files. Molecular docking studies were performed using GOLD version 5.2.2 in which the target atoms are fixed and the ligands are flexible [45]. The GoldScore scoring function was employed for the ranking of molecules according to their score which is given as fitness. Best cluster poses were saved and visually analyzed by PyMol version 2.2.3 [46] and Maestro version 11.3 of the Schrodinger suite [43].

3. Results and discussion

3.1. Chemistry

3.1.1. Preparation of 3,5-dimethylbenzimidazolium salts 2a–f

The 3,5-dimehylbenzimidazolium salts **2a-f** were synthesized *via* two *N*-alkylation reaction processes as illustrated in scheme 1. Compound **1** as a starting material was obtained by the first *N*-alkylation reaction using 5,6-dimethylbenzimidazole with bromodiphenylmethane. The second *N*-alkylation reaction allowed us to prepared six benzimidazolium salts **2a-f** by reacting *N*-benzhydryl-5,6-dimethylbenzimidazole **1** with different benzyl chloride in degassed DMF at 80 °C. All the new 3,5-dimehylbenzimidazolium salts **2a-f** were obtained with good yield, in the solid-state.

All the new 3,5-dimehylbenzimidazolium salts **2a-f** depicted in Scheme 1 were obtained with good yield. The spectroscopic data of 3,5-dimethylbenzimidazolium salts are consistent with the data observed in literature for other benzimidazolium salts [7,9-12]. The physical and some spectroscopic data of 3,5-dimethylbenzimidazolium salts are summarized in Table 2.

These new 5,6-dimethylbenzimidazolium salts were characterized by different techniques. The FT-IR data indicated that 5,6-dimethylbenzimidazolium salts show a characteristic $\nu_{(CN)}$ band typically for all salts **2a-f** at 1549, 1548, 1546, 1541, 1542, and 1552 cm^{-1} respectively. In ^{1}H NMR the important pick for all 3,5-dimethylbenzimidazolium salts is

Table 2
Physical and Spectroscopic data for 3,5-dimethylbenzimidazolium salts **2a-f.**

Code	Chemical Formula	Molecular Weight (g/mol)	Melting point°C	^{1}H NMRCH (C_2) ppm	^{13}C NMR(C_2) ppm	IR$\nu_{(CN)}$
2a	$C_{33}H_{36}ClN_2$	495.11	153	10.52	142.3	1549
2b	$C_{30}H_{29}ClN_2$	453.03	260	11.27	142.6	1548
2c	$C_{32}H_{33}ClN_2$	481.08	156	10.91	142.8	1546
2d	$C_{30}H_{29}ClN_2$	453.03	152	11.15	142.5	1541
2e	$C_{33}H_{35}BrN_2$	539.56	180	10.75	141.6	1542
2f	$C_{32}H_{33}ClN_2O_3$	529.08	158	11.27	142.7	1552

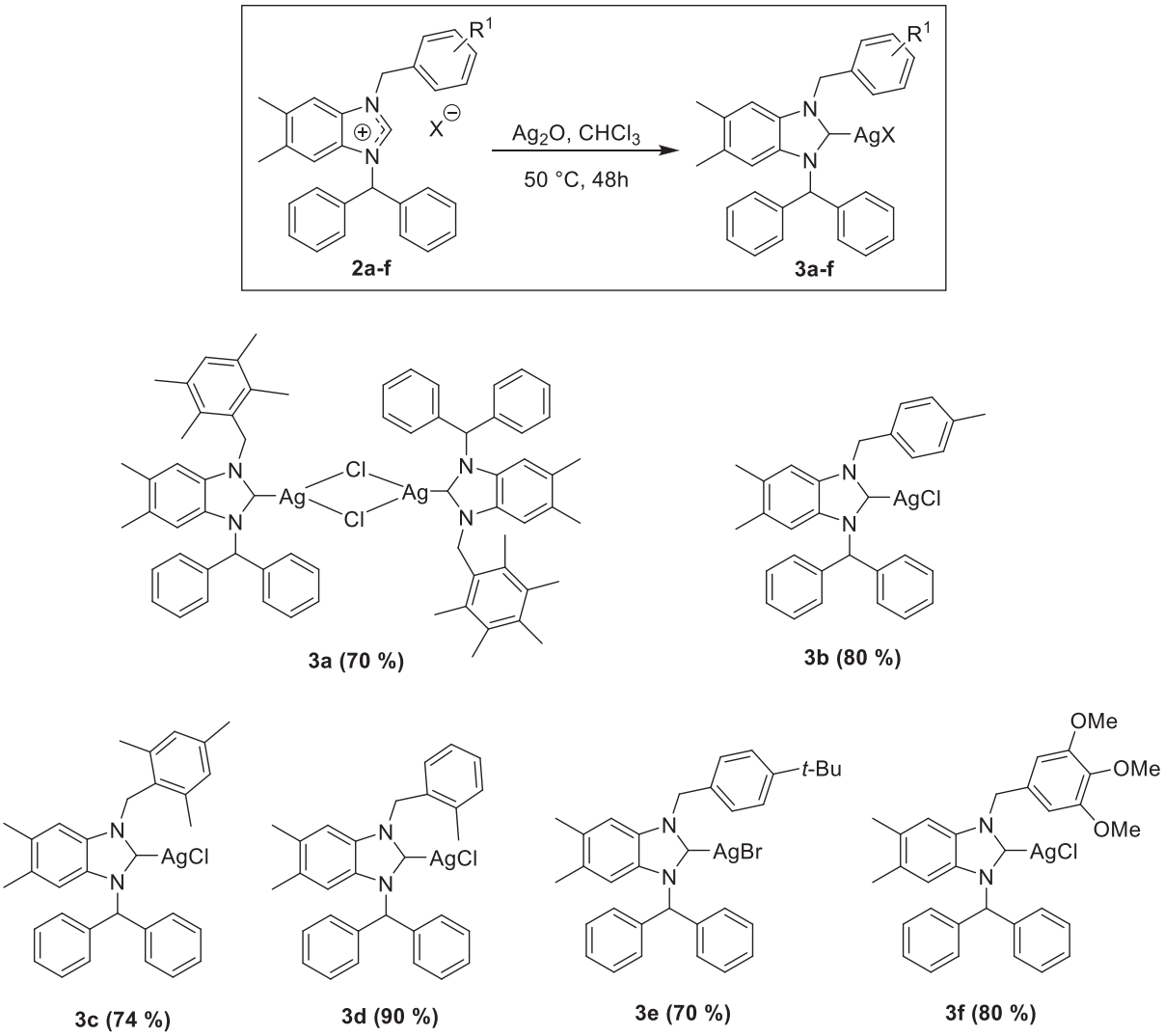

Scheme 2. Synthesis of Ag(I)–NHC complexes **3a-f**.

Table 3
Physical and Spectroscopic data for Ag(I)–NHC complexes.

Code	Chemical Formula	Molecular Weight (g/mol)	Melting point °C	^{1}H NMR*CH* (C_2) ppm	^{13}C NMR (C_2) ppm	IR $\nu_{(CN)}$
3a	$C_{32}H_{34}AgClN_2$	601.97	245–246	–	–	1471
3b	$C_{30}H_{28}AgClN_2$	559.89	144–145	–	–	1484
3c	$C_{32}H_{32}AgClN_2$	584.97	200–201	–	–	1496
3d	$C_{30}H_{28}AgClN_2$	559.89	222–223	–	–	1485
3e	$C_{33}H_{34}AgBrN_2$	646.42	218–219	–	–	1481
3f	$C_{32}H_{33}AgClN_2O_3$	635.94	117–118	–	–	1505

the pick of the acidic proton NC*H*N that confirms the formation of the salt, this pick was detected at 10.52, 11.25, 10.91, 11.08, 10.73, and 11.25 ppm respectively for the salts **2a-f**, as sharp singlets. In ^{13}C NMR the carbon NC*H*N was observed as typical singlets at 142.4, 142.7, 142.8, 142.5, 141.6, and 142.7 ppm respectively for the salts **2a-f**.

3.1.2. Preparation of silver(I)–NHC complexes 3a-f

The Ag(I)–NHC complexes **3a-f** were synthesized *via* the in situ deprotonation of 3,5-dimethylbenzimidazolium salts by Ag_2O. Treatment of the benzimidazolium salts with Ag_2O in dichloromethane at room temperature in the dark afforded the expected silver complexes Ag(I)–NHC **3a-f** (Scheme 2). The silver-NHC complexes **3a-f** were obtained as white solids in high yields, soluble in halogenated solvents. In the air, these complexes are stable but are light-sensitive.

All the new Ag(I)–NHC complexes **3a-f** depicted in Scheme 3 were obtained with good yield. The spectroscopic data of these complexes are consistent with the data observed in literature for other Ag(I)–NHC complexes [9–12]. The physical and some spectroscopic data are summarized in Table 3.

These new six Ag(I)–NHC complexes were characterized by different techniques. The FT-IR data indicated that Silver(I)–NHC complexes show a characteristic $\nu_{(CN)}$ band typically for all complexes **3a-f** at 1471, 1484, 1496, 1485, 1481, and 1505 cm^{-1} respectively. The characteristic proton peak NC*H*N of the starting benzimidazolium was not detected in

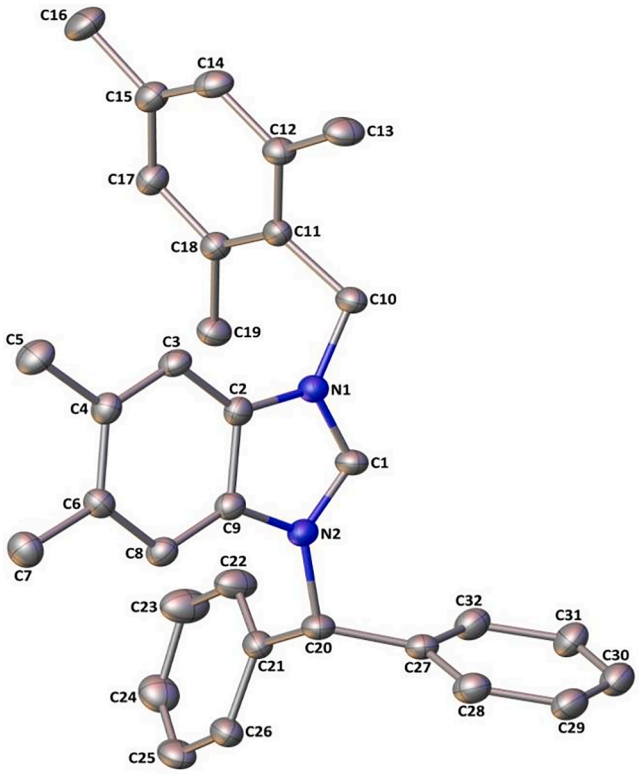

Fig. 1. Molecular structure of salt **2c**.

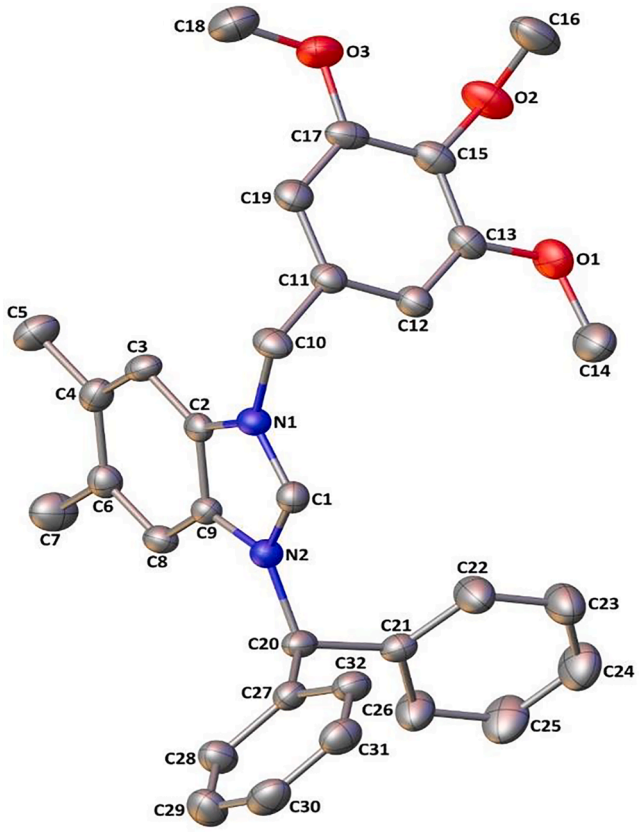

Fig. 2. Molecular structure of salt **2f**.

the ^{1}H NMR spectra of novel Ag(I)–NHC complex that confirmed the formation of the Ag(I)–NHC complexes Table 3. Similarly, in the ^{13}C NMR data, the characteristic signals of carbon NCHN were observed at around 144 ppm for the starting benzimidazolium salts. However, the formation of silver NHC complexes is checked by the disappearance of the signal of NCHN.

3.2. *X-ray crystal structures*

The molecular diagrams of **2c**, **2f,** and **3a** with the adopted atom-labeling scheme are shown in Figs. 1-3, while important bond distances and angles are listed in Table 4.

3.2.1. *Description of the structure of the salts 2c and 2f*

The 3,5-dimethylbenzimidazolium salts **2c** and **2f** crystallize in chloroform/diethyl ether as depicted in Figs. 1 and 2.

The compounds **2c** and **2f** crystallize as a salt in which the charge of the NHC cation is neutralized by a chloride anion. Furthermore, in their asymmetric units, **2c** contains two solvent water molecules whilst **2f** contains one dichloromethane molecule. The bonding within the imidazole rings indicates a pattern of delocalization that extends from atom N1 to atom N2 through atom C1, the N1—C1 and N2—C1 distances being significantly shorter than the N1—*C*2 and N2—C9 distances. The remaining bond lengths are normal within experimental uncertainty [47].

3.2.2. *The structure description of the silver complex 3a*

The silver(I)NHC complex **3a** crystallizes in chloroform/diethyl ether as depicted in Fig. 3.

The silver(I)–NHC complex **3a** crystallizes as dimers *via* bridging chloride atoms to form an $Ag_2(\mu\text{-}Cl)_2$ quadrangular arrangement which is frequently observed in silver complexes (Fig. 3). Because of the inversion center, the Ag_2Cl_2 cluster is strictly planar at the mid-point of the Ag···Ag^{i} line [symmetry code: $^{i} -x + 1/2, -y + 3/2, -z + 1$], where each silver(I) atom is tri-coordinated with one carbene carbon atom and two chlorine atoms to adopt a distorted trigonal planar geometry. The two (NHC)AgCl moieties are present around an inversion center with the chlorides asymmetrically bound to the silver center with different Ag—Cl bond lengths of 2.464(2) and 2.629(2) Å. The Ag1—C1 distance of 2.111(8) Å falls in the range typical for other silver-carbene complexes [48]. With an angle of 143.2(2)° the C—Ag—Cl vector deviates from linearity as a result of coordination from an additional bridging Cl. The bond angles of the C1—Ag1—Cl1^{i}, Ag1—Cl11—Ag1^{i,} and Cl1—Ag1—Cl1^{i} are 124.1(2), 87.34(7), and 92.66(7)°, respectively. The Ag…Ag distance is 3.5186(11) Å, much greater than the sum of two van der Waals radii for Ag (3.44 Å) [49], ruling out the presence of any 'argentophilic' interaction. Due to coordination of the NHC ligand, the ring's internal angle (N1—C1—N2) is reduced at the carbene center from 109.2(6) to 106.2(7)°. All the aforementioned data are comparable to those reported dinuclear Ag(I)–NHC complexes [50–54].

3.3. *Evaluation of biological*

3.3.1. *Evaluation of antibacterial activity*

Investigations have been performed for antibacterial and antifungal activities *in vitro* against (E.coli, P.aeruginosa, S.aureus, C.albicans, and C.glabrata) for all the newly 3.5-dimethylbenzimidazolium salts **2a-f** and their related silver(I)–NHC complexes **3a-f,** using AmphotericinB, Voriconazole, Ampicillin, and Tetracycline as a standard control drug. The (MIC μg/mL) results of the antimicrobial activity of all new compounds are reported in Table 5.

Globally, all benzimidazoluim salts and silver-NHC complexes tested showed an important antifungal activity against the human pathogenic microorganisms (*Candida albicans* and *Candida glabrata*) as are presented in Table 4. The benzimidazolium salts **2a-f** showed high antifungal activity against Candida albicans, especially the three salts **2a**, **2c**, and **2e**.

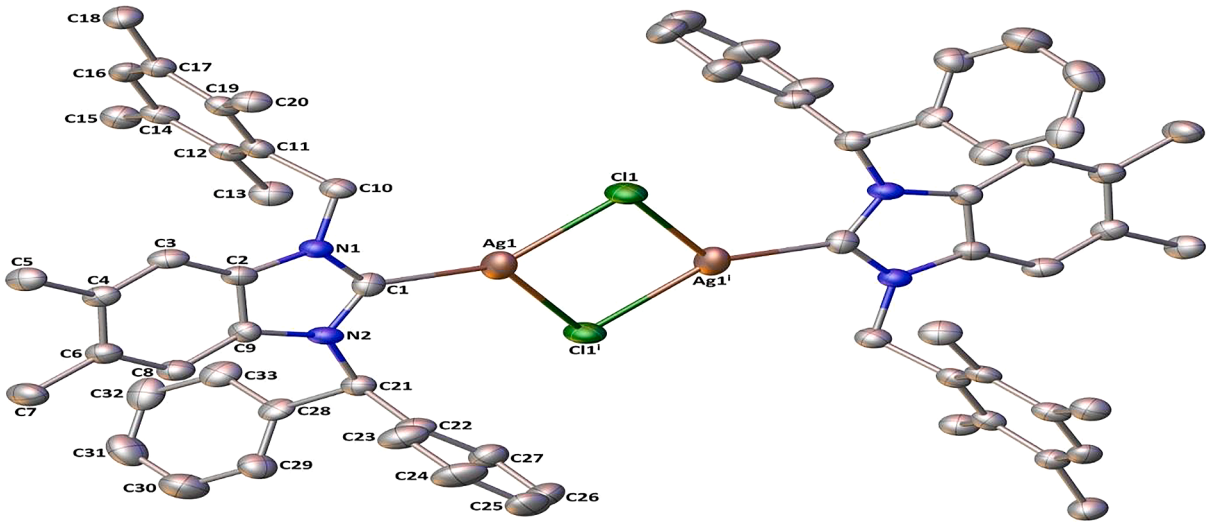

Fig. 3. Molecular structure of silver-carbene complexes **3a**.

Table 4
Selected geometric parameters for **2c**, **2f**, and **3a**.

Parameters		3,5-Dimethylbenzimidazolium salts		Silver(I)–NHC complex
		2c	2f	3a
Bond lengths (Å)	Ag1—Cl1	–	–	2.464(2)
	Ag1—Cl1^{i}	–	–	2.629(2)
	Ag1—C1	–	–	2.111(8)
	N1—C1	1.351(7)	1.322(4)	1.342(9)
	N1—C2	1.392(7)	1.392(5)	1.390(9)
	N2—C1	1.341(7)	1.334(5)	1.355(10)
	N2—C9	1.406(8)	1.398(5)	1.391(9)
Bond angles (°)	Cl1—Ag1—C1	–	–	143.2(2)
	Cl1^{i}—Ag1—C1	–	–	124.1(2)
	Cl1—Ag1—Cl1^{i}	–	–	92.66(7)
	Ag1—Cl1—Ag1^{i}	–	–	87.34(7)
	Ag1—C1—N1	–	–	125.7(6)
	Ag1—C1—N2	–	–	127.9(6)
	N1—C1—N2	109.2(6)	110.5(3)	106.2(7)
	C1—N1—C2	109.6(5)	108.4(3)	111.4(7)
	C1—N2—C9	110.1(5)	107.6(3)	110.4(6)

Symmetry code: $^{i} -x + 1/2, -y + 3/2, -z + 1$.

besides, the silver-NHC complex **3a-f** showed high antifungal activity against *Candida albicans*, and *Candida glabrata*, with almost the same values. Complex **3c** is the more active complex. The antibacterial activity of all benzimidazoluim salts **2a-f** and silver-NHC complexes **3a-f** tested showed an important antibacterial activity against the human pathogenic microorganisms (*Escherichia coli*, *Pseudomonas aeruginosa*, and *Staphylococcus aureus*), except the salt **2f** as are presented in Table 4. All benzimidazolium salts **2a-e** showed good antibacterial activity against *Staphylococcus aureus* and *Escherichia coli,* with almost the same values, but they didn't show high activity against *Pseudomonas aeruginosa* especially for the two salts **2b**, and **2d** the last salt **2f** didn't show any activity against E. coli. In contrast, the silver-NHC complexes **3a-f** showed high antimicrobial activity against Staphylococcus aureus and Escherichia coli. The results revealed that the highest antimicrobial activity was reported in Ag-NHC complexes **3b** and **3c**.

The lipophilicity of Ag(I)–NHC complexes are thought to play a significant role in the ability of these compounds to penetrate cellular membranes, and increased lipophilicity through modification of the NHC wingtip substituents improved the antibacterial activity of compounds [55-57].

3.3.2. *Enzymatic inhibitory activity assay*

The inhibitory effect of all benzimidazolium salts **2a-f** and their silver(I)NHC complexes **3a-f** against different enzymes as AChE, BChE, Lipase, and α-amylase was studied *in vitro* at different concentrations. The benzimidazolium salts and their silver complexes demonstrated close percentages of inhibition against AChE compering with the standard Galanamine, while against BChE, all newly compound inhibited more effectively than the standard drug. The inhibitory effect of silver complexes against lipase showed that all compounds **3a-f** could effectively inhibit lipase with a value of IC_{50} approximates the standard (Orlistat). Also, this series of silver complexes exhibited strong and good anti-diabetic activity against the α-amylase enzyme. Contrary to these results, all benzimidazolium salts didn't show any activity against both lipase and α-amylase enzymes. Enzymatic activity was reported in the same manner as IC_{50} values presented in Table 6. Based on the IC_{50} values, the results were given as a concentration of 50% inhibition (IC_{50}). The inhibition of different enzymes was determined by comparing the reaction rates of samples relative to the blank sample. The capacity of the newly synthesized compound to inhibit the enzymes (AChE, BChE, Lipase, and α-amylase) was evaluated according to the spectrophotometric methods. The low IC_{50} values designated the high inhibition activity.

A. Evaluation of Acetylcholinesterase and Butyrylcholinesterase inhibitory capacity

To find out the capacity of both benzimidazolium salts **2a-f** and their silver(I)–HNC complexes **3a-f** against anticholinesterase activity, all the compounds were screened in an *in vitro* complementary system. Acetylcholinesterase (AChE) and butyrylcholinesterase (BChE) are the enzymes that catalyze the hydrolyses of substrate acetylthiocholine or butyrylthiocholine, respectively. The product thiocholine reacts with Ellman's reagent (DTNB) to produce 2- nitrobenzoic-5-mercaptothiocholine and 5-thio-2-nitrobenzoate which can be detected at 412 nm. For comparison purposes, Galantamine, a medicinal cholinesterase inhibitor used in mild Alzheimer's disease treatment, was used as the positive control.

As can be seen in Table 6, The obtained IC_{50} values revealed that all tested compounds showed a strong inhibitory against both enzymes. (AChE and BChE) with IC_{50} values ranging from (IC_{50}: 1.33 ± 0.3 μM to 17.97 ± 0.27 μM). The best AChE inhibitors between all compounds are **2a** for salts with (IC_{50}: 1.33 ± 0.3 μM), and **3a** for their silver(I) complexes with (IC_{50}: 1.60 ± 0.19 μM) comparing to that of the Galantamine (4.14 ± 0.07 μM). The compound **2f** is the least active AChE inhibitor

Table 5
Antifungal and anti-Bacterial activities (MIC $\mu g/mL$) of benzimidazolium salts **2a-f** and their silver(I)NHC complexes **3a-f.**

Compounds		*Anti-Fungal*		*Anti-Bacterial*		
		C. albicans[a]	C. glabrata[a]	E. coli[a]	P. aeruginosa[a]	S. aureus[a]
Benzimida-zolium Salts	2a	25	100	200	200	200
	2b	200	200	400	800	400
	2c	25	100	200	200	200
	2d	100	200	400	800	400
	2e	12.5	100	200	200	100
	2f	200	400	NA	NA	NA
Silver complexes	3a	12.5	12.5	25	50	25
	3b	12.5	12.5	25	25	6.25
	3c	6.25	6.25	25	25	6.25
	3d	12.5	12.5	25	50	12.5
	3e	12.5	12.5	25	25	12.5
	3f	25	12.5	25	50	25
	Ampicillin[b]	–	–	12.5	400	3.125
	Tetracycline[b]	–	–	0.8	12.5	0.2
	Amphotericin B[b]	0.05	0.1	–	–	–
	Voriconazole[b]	0.4	0.4	–	–	–

a: Tested microorganisms.
b: Reference drugs.
NA: Not Active.

Table 6
Anti-Cholinesterase, anti-Lipase, and Anti-α-Amylase activities of benzimidazolium salts **2a-f** and their silver(I)–NHC complexes **3a-f.**

Compound		Anti-Cholinesterase AChE $IC_{50} \pm SD$ (μM)[a]	Anti-Cholinesterase BChE $IC_{50} \pm SD$ (μM)[a]	Anti-Lipase Lipase $IC_{50} \pm SD$ (μM)[a]	Anti-α-Amylase α-amylase $IC_{50} \pm SD$ (μM)[a]
Benzimidazolium salts	**2a**	1.33 ± 0.03	0.96 ± 0.02	NA[c]	NA[c]
	2b	5.56 ± 0.57	0.72 ± 0.04	NA[c]	NA[c]
	2c	6.17 ± 0.33	0.70 ± 0.04	NA[c]	NA[c]
	2d	4.19 ± 0.02	0.15 ± 0.02	NA[c]	NA[c]
	2e	9.06 ± 0.26	1.08 ± 0.12	NA[c]	NA[c]
	2f	17.97 ± 0.27	4.29 ± 0.18	NA[c]	NA[c]
Silver(I)–NHC complexes	**3a**	1.60 ± 0.19	0.88 ± 0.00	33.79 ± 6.17	7.00 ± 0.87
	3b	3.50 ± 0.52	0.47 ± 0.04	52.25 ± 1.83	70.69 ± 2.69
	3c	5.64 ± 0.02	0.50 ± 0.03	34.61 ± 2.50	98.57 ± 2.18
	3d	4.21 ± 0.12	0.61 ± 0.02	40.72 ± 2.47	43.18 ± 2.60
	3e	4.53 ± 0.13	0.18 ± 0.01	33.15 ± 1.47	65.87 ± 2.66
	3f	4.14 ± 0.46	3.57 ± 0.15	58.66 ± 1.47	47.55 ± 1.28
Reference	**Galanamine[b]**	4.14 ± 0.07	20.38 ± 2.10	/	/
	Orlistat [b]			25.07 ± 0.48	
	Acarbose [b]	/	/	/	5258.02 ± 46.9

a: IC_{50} values represent the means ± SD of three parallel measurements ($p < 0.05$).
b: Reference compound.
c: Not Active.

with (IC_{50}: 17.97 ± 0.27 μM) between all salts. While compound **3c** is the least active AChE inhibitor with (IC_{50}: 5.64 ± 0.02 μM**)** between the silver(I) complexes. It should be noted that compounds **2d, 3d, 3e,** and **3f** showed IC_{50} values in the same range of the standard Galantamine. Accordingly, benzimidazolium salts and silver (I)–NHC complexes could be considered promising acetylcholinesterase inhibitors. According to Taylor et al [58]. The compounds that give a good inhibitory activity of acetylcholinesterase (AChE) are more beneficial for human health.

The data obtained for inhibition of BChE by benzimidazolium salts (**2a-f**) and their silver(I)–NHC complexes (**3a-f**) demonstrated that all compounds had high activity toward BChE. In terms of anti-BChE activity, the inhibitory potencies of all compounds toward BChE with IC_{50} values ranging from (IC_{50}: 0.29 ± 0.04 μM to 4.29 ± 0.18 μM**),** with IC_{50} values ranging from (IC_{50}: 0.29 ± 0.04 μM to 4.29 ± 0.18 μM). The most active benzimidazolium salts were **2d** with (IC_{50}: 0.15 ± 0.02 μM). The most active silver (I)–NHC complexes were **3e** with (IC_{50}: 0.18 ± 0.01 μM). The benzimidazolium salt **2f** and their silver(I) complex **3f** are the least active BChE inhibitor with (4.29 ± 0.18 μM) and (3.57 ± 0.15 μM) respectively. On the other hand, compared with galantamine standard. All-new compounds were more potent than the standard drug galantamine against the BChE enzyme. Generally, the inhibition of BChE by the benzimidazolium salt and their silver(I)–NHC complexes were more efficient than the AChE inhibitor activity. It was also noted that all compounds were more selective for BChE than the standard drug Galantamine. The selectivity was especially pronounced for compounds **2c**, **2d**, **2e**, **3c**, **3d**, and **3e.** The performance for the compound **3d** was 30.07-fold more selective for BChE. While for AChE inhibitors, all compounds had less affinity than Galantamine.

As presented in Table 7, the compounds Ag(II)–NHC complexes **3a-f** are polar molecules, these compounds present high log P values superior to 5 (log P > 5), which means that these compounds are too lipophilic (poor aqueous solubility). The benzimidazolium slats **2a-f** have a good aqueous solubility because of their log P value which included between 0 and 5. The standard (Galantamine**)** has log P values inferior to 3 (log P = -1.42) which has low partition coefficients. This compound is a polar molecule whith a good aqueous solubility.

B. Evaluation of Pancreatic Lipase inhibitory capacity.

The inhibitor of digestive lipase that limits intestinal fat absorption at an initial stage could prove as a proper medication for the treatment of hyperlipidemia and holds great promise as an anti-obesity agent. To find new pancreatic lipase (triacylglycerol lipase, EC 3.1.1.3) inhibitors from these new compounds, all the 3,5-dimethylbenzimidazolium salts **2a-f** and the related silver(I)–NHC complexes **3a-f** were tested for their anti-

Table 7
The selectivity index for AChE over BChE and BChE over AChE with docking score and log P of benzimidazolium salts **2a-f** and their silver(I)–NHC complexes **3a-f.**

Compounds		AChE			BChE			
		$IC_{50} \pm SD$ (μM)[a]	Selectivity index[c]	Docking score	$IC_{50} \pm SD$ (μM)[a]	Selectivity index[d]	Docking score	Log P
Benzimidazolium salts	**2a**	1.33 ± 0.03	0.72	59.20	0.96 ± 0.02	1.38	74.74	5.17
	2b	5.56 ± 0.57	0.13	54.43	0.72 ± 0.04	7.72	76.60	5.04
	2c	6.17 ± 0.33	0.11	51.78	0.70 ± 0.04	8.81	76.71	4.80
	2d	4.19 ± 0.02	0.06	56.48	0.15 ± 0.02	14.45	77.60	4.00
	2e	9.06 ± 0.26	0.11	52.73	1.08 ± 0.12	8.39	70.26	5.30
	2f	17.97 ± 0.27	0.23	51.65	4.29 ± 0.18	4.18	68.27	3.23
Silver complexes	**3a**	1.60 ± 0.19	0.55	59.11	0.88 ± 0.00	1.82	74.98	8.40
	3b	3.50 ± 0.52	0.13	58.43	0.47 ± 0.04	7.44	77.12	7.46
	3c	5.64 ± 0.02	0.08	53.04	0.50 ± 0.03	11.28	76.80	8.19
	3d	4.21 ± 0.12	0.14	56.22	0.61 ± 0.02	30.07	76.58	7.41
	3e	4.53 ± 0.13	0.07	56.87	0.18 ± 0.01	12.94	77.10	8.62
	3f	4.14 ± 0.46	0.86	57.09	3.57 ± 0.15	1.16	70.15	6.64
	Galantamine [b]	4.14 ± 0.07	4.92	57.02	20.38 ± 2.10	0.20	53.04	−1.42

c : Selectivity for AChE: IC_{50}(BChE)/IC_{50}(AChE).
d: Selectivity for BChE: IC_{50}(AChE)/IC_{50}(BChE)

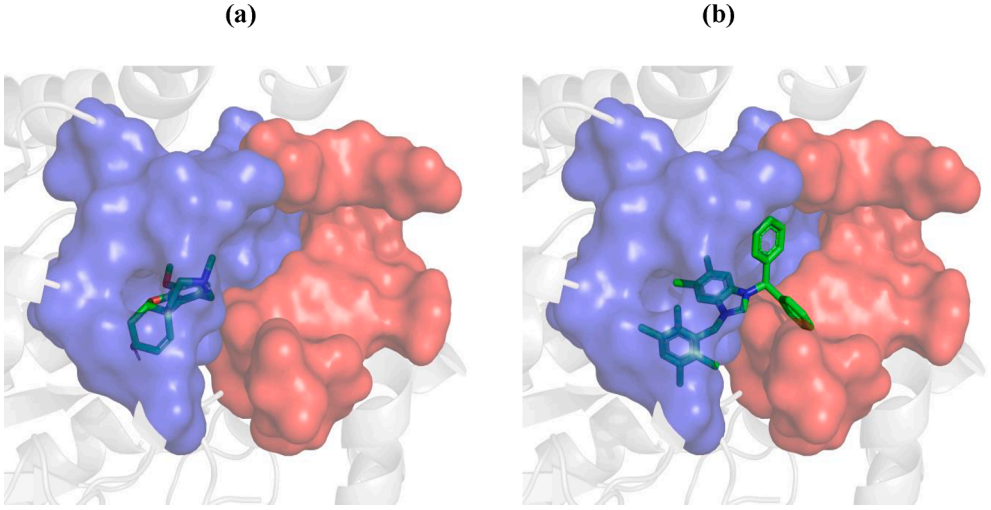

Fig. 4. The positioning of galantamine **(a)** and, **2a (b)** in the AChE active site.

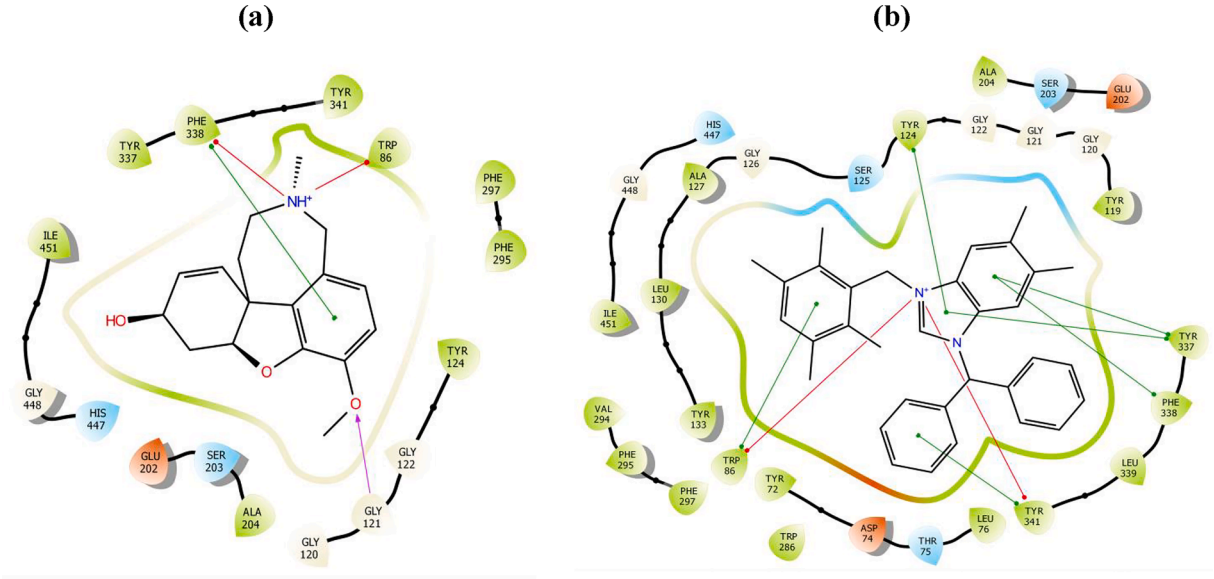

Fig. 5. Binding mode prediction of galantamine **(a),** and compound **2a (b)** into the entire AChE active pocket.

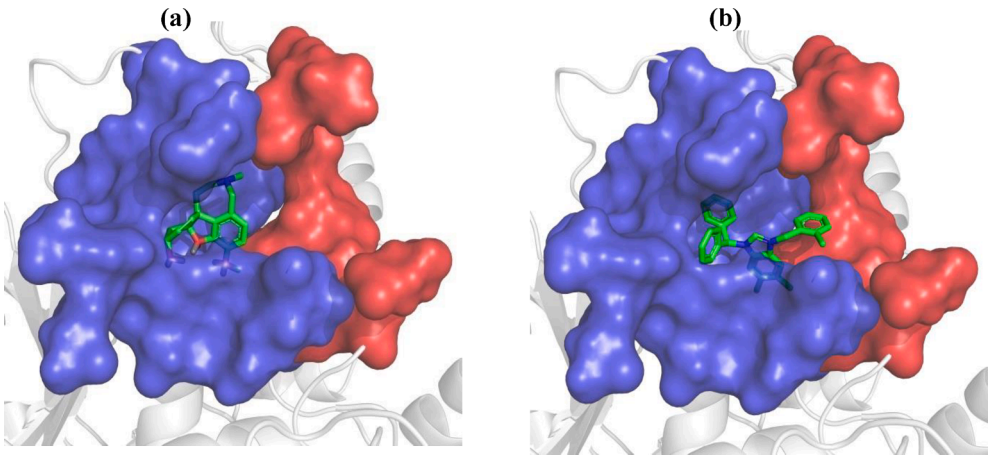

Fig. 6. The positioning of galantamine **(a),** and **2d (b)** in BChE active site.

lipase activity using a radioactive screening method. The results shown in Table 5 represent a significant inhibitory activity against Lipase by all the silver complexes, especially the complexes **3a** and **3e** that displayed remarkable anti-lipase activity with (IC_{50} = 33.79 ± 6.17 μM) and (IC_{50} = 33.15 ± 1.47 μM) respectively, were found to be very close to the reference drug orlistat (IC_{50} = 25.07 ± 0.48 μM). Opposite of that, all salts **2a-f** were not active against the lipase enzyme. This study proved that Ag's presence in the compound gave the capacity for the complexes to had anti-lipase activity.

C. Evaluation of α-amylase inhibitory capacity

The evaluation of 3,5-dimethylbenzimidazolium salts and their silver (I)–NHC complexes effect were tested using α-amylase inhibitory assay; the study was investigated the anti-diabetic activity of these new compounds. As shown in table 5. The α-amylase inhibitor effects of silver (I)–NHC complexes showed higher inhibitory activity than acarbose (IC_{50} = 5258.02 ± 4.9 μM). The greatest α–amylase inhibition activity was obtained in the compound **3a**, with (IC_{50} = 7.00 ± 0.87 μM). While all benzimidazolium salts **2a-f** are not active against α–amylase. They didn't show any anti-diabetic activity.

3.4. Molecular docking study

Molecular docking studies were carried out to get a better insight into the binding modes and amino acid interactions of the synthesized compounds into AChE and BChE actives sites. Table 7 reveals that the experiment data of enzyme inhibitory activity *in vitro* showed that the molecular docking findings were in good agreement. Indeed, the most potent inhibitors from *in vitro* assays showed the best docking scores against both enzymes. The most promising compounds (compound **2a** for AChE and **2d** for BChE) were chosen to be investigated further of their binding mode with their target. As shown in Fig. 4, compound **2a** covers both the catalytic anionic site (CAS) and the peripheral anionic site (PAS) of AChE, leading to an inhibitory potency 3 fold more than that of galantamine, which binds only to the CAS. Also, The disparity in inhibitory potency between these two compounds may be explained by the different number of interactions between them and the protein (Fig. 5). Indeed, whereas **2a** is involved in eight interactions (six π-π stacking with Trp86, Tyr124, Tyr337, Phe338, Tyr341, and two π-cation interactions with Trp86 and Tyr341), galantamine is involved in only four interactions (two π-cation interactions with Trp86 and Phe338, a hydrogen bond with Gly121 and a π-π stacking with Phe338).

The most plausible pose of each compound is presented as obtained by docking with Gold. Residue Tyr341, which protects the pocket's ligand, is omitted for clarity. The CAS area of the cavity is shown in blue,

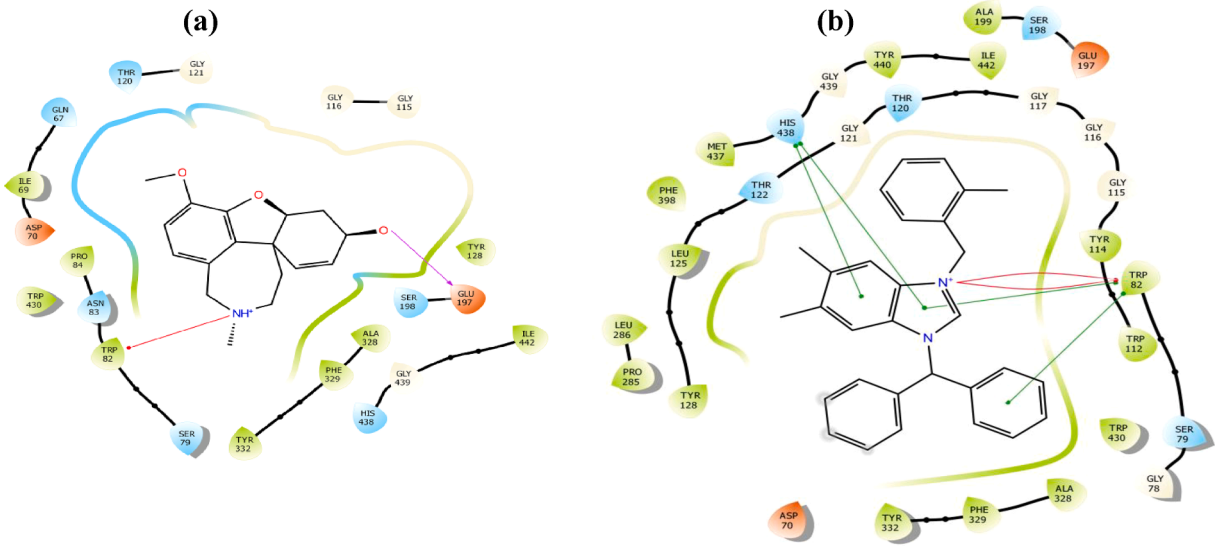

Fig. 7. Binding mode prediction of galantamine **(a)** and compound **2d (b)** into the entire BChE active pocket.

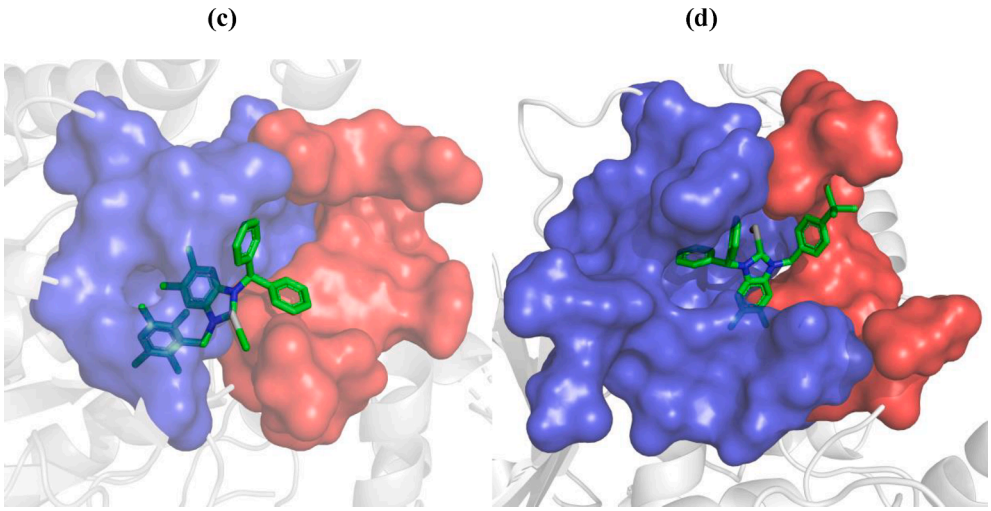

Fig. 8. The positioning of complex **3a (c)** in AChE, and **3e (d)** in BChE active sites.

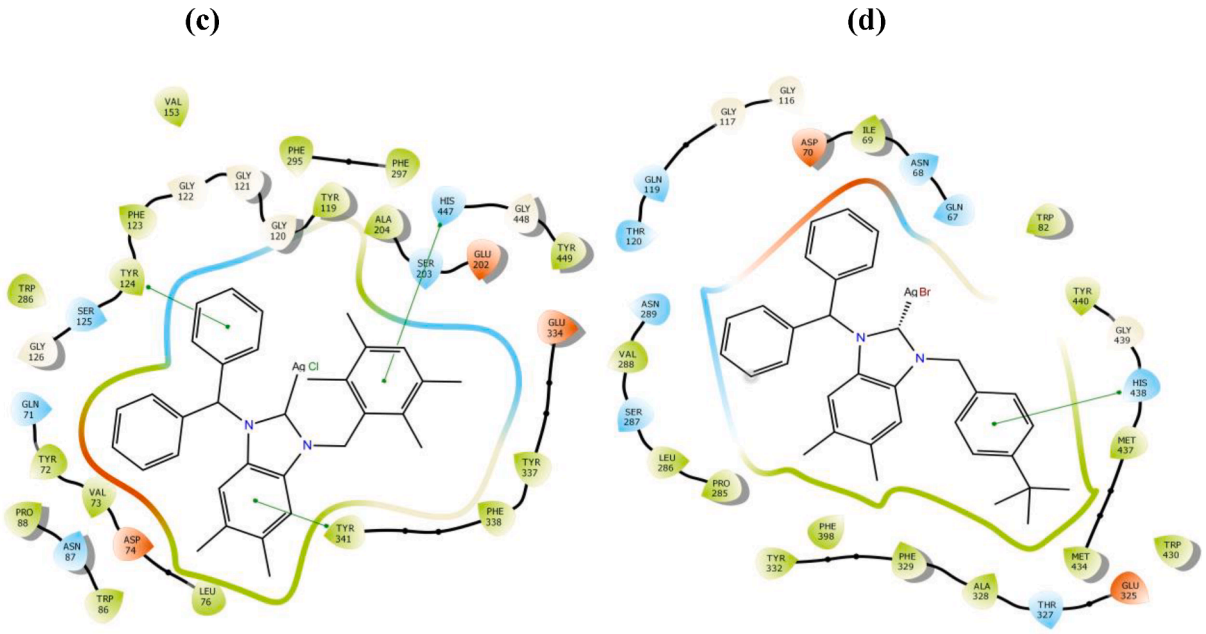

Fig. 9. Binding mode prediction of compound **3a (c)** and compound **3e (d)** into the entire AChE and BChE active pocket.

while the PAS is shown in red. The ligand atoms are color-coded as follows: oxygen in red, carbon in green, and nitrogen in blue. The images were drawn by PyMol.

Purple arrows head from the donor to the acceptor of hydrogen bonds, red lines represent π-cation interactions, and green lines π-π stacking. The images were done with the Ligand Interaction Diagram script from the Schrödinger Suite.

Concerning the BChE, The inhibitory potency of compound **2d** is higher than that of galantamine. because of its rational positioning in this enzyme's binding site. Indeed, compound **2d** binds both the CAS and PAS of BChE in contrary to galantamine which covers only the CAS (Fig. 6). Also, **2d** establishes a higher number of interactions against BChE active site than that of galantamine (Fig. 7). Indeed, whereas galantamine is involved in only two interactions (hydrogen bond with Glu197 and π-cation interaction with Trp82), **2d** is involved in six interactions of which two π-π stackings with His438. This residue was described to play an important role in the BChE activity [39]. Fig. 8. Fig. 9.

Remarkably, salts are more powerful compared to complexes since the positively charged nitrogen of the cycle engages in the formation of π -cation bonds with the residues of the active site of the enzyme (Trp86 in the case of AChE and Trp82 in the case of BChE) which increases the affinity of the salts, as for **2a** and **2d** compared to their silver(I)–NHC complex analog (**3a** and **3d**) against AChE and BChE respectively. This increase of the inhibitory potency may be explained by the formation of a π-cation interaction between the nitrogen of salts, and Trp86 for AChE (Trp82 for BChE). As shown in (Figure 08 (c)) , the Ag(II)NHC complex **3a** forms three π-π stackings with Tyr124, Tyr341 and His447 of AChE active site. The absence of π-cation with Trp86 seems to decrease its affinity compared to its salt analog **2a**. Likewise, the absence of π-cation with Trp82 seems to decrease the affinity of silver(I)–NHC complexes against BChE, as for **3e** establishes a π-π stacking with His438 of BChE active site (Figure 08 (d)).

4. Conclusion

In this research, six benzimidazolium salts and their related silver(I)–NHC complexes have been synthesized and identified with different spectroscopic analysis methods. All selected compounds were tested for their biological capacity using anti-microbial, anti-cholinesterase, anti-α-amylase, and anti-lipase activities. Importantly, our results provide evidence for showing the best results comparing with the reference standard control drug. The silver(I)–NHC complexes showed important anti-microbial activity and significate inhibitory against all types of enzymes, such as AChE, BChE, α-amylase, and lipase. Contrary to this the benzimidazolium salts showed a moderate anti-microbial activity and the inhibition by enzymes was recorded just for AChE and BChE. A great correlation between experimental and theoretical studies for these new compounds was obtained by molecular docking study. Based on our findings, the synthesis of Ag-NHC complexes allowed us to confirm that the use of Ag as a metal with NHCs increase the biological activity, which made silver(I)–NHC complexes considered as metallopharmaceutical compound par excellence to be used in the medicine and pharmaceutical industries, and provide promising starting points for further research to develop new drugs for the treatment of many diseases.

Declaration of Competing Interest

The authors declare that they have no known competing financial interests or personal relationships that could have appeared to influence the work reported in this paper.

Acknowledgments

The authors greatly acknowledge financial support from the İnönü University Research Fund of this work. X-ray analyses were supported by the Scientific Research Projects Unit of Ondokuz Mayıs University (Project No: PYO.FEN.1906.19.001).

Appendix A. Supplementary data

Supplementary data to this article can be found online at https://doi.org/10.1016/j.ica.2021.120486.

References

[1] R. Kılınçarslan, N. Sadıç, Catalytic activity of N-heterocyclic carbene silver complexes derived from imidazole ligands, Inorganic and Nano-Metal Chemistry 47 (3) (2017) 462–466, https://doi.org/10.1080/15533174.2016.1186054.
[2] F.E. Hahn, M. Jahnke, Heterocyclic carbenes: Synthesis and coordination chemistry, Angewandte Chemie - International Edition 47 (17) (2008) 3122–3172, https://doi.org/10.1002/(ISSN)1521-377310.1002/anie.v47:1710.1002/anie.200703883.
[3] R.A. Haque, N. Hasanudin, M.A. Iqbal, A. Ahmad, S. Hashim, A. Abdul Majid, M.B. K. Ahamed, Synthesis, crystal structures, in vitro anticancer, and in vivo acute oral toxicity studies of bis-imidazolium/benzimidazolium salts and respective dinuclear Ag(I)- N -heterocyclic carbene complexes, J. Coord. Chem. 66 (18) (2013) 3211–3228, https://doi.org/10.1080/00958972.2013.831406.
[4] I. Özdemir, S. Demir, S. Günal, I. Özdemir, C. Arici, D. Ülkü, Synthesis, characterization and antimicrobial activity of new silver complexes with N-heterocyclic carbene ligands, Inorg. Chim. Acta 363 (14) (2010) 3803–3808, https://doi.org/10.1016/j.ica.2010.07.034.
[5] İ. Özdemir et al., "Synthesis, characterization and antitumor properties of novel silver(I) and gold(I) N-heterocyclic carbene complexes," Inorganica Chimica Acta, vol. 506, no. February, 2020, doi: 10.1016/j.ica.2020.119530.
[6] M.U.M. Ulu, E. Evren, N. Gürbüz, İ.Ö.İ. Özdemir, N. Hamdi, İ. Özdemir, Rhodium (I) N-heterocyclic carbene Complexes: Synthesis and cytotoxic Properties, New J. Chem. (2021).
[7] N. Şahin, S. Şahin-Bölükbaşı, M.N. Tahir, C. Arıcı, E. Çevik, N. Gürbüz, İ. Özdemir, B.S. Cummings, Synthesis, characterization and anticancer activity of allyl substituted N-Heterocyclic carbene silver(I) complexes, J. Mol. Struct. 1179 (2019) 92–99, https://doi.org/10.1016/j.molstruc.2018.10.094.
[8] E. Meggers, "Targeting proteins with metal complexes," pp. 1001–1010, 2009, doi: 10.1039/b813568a.
[9] T.J. Siciliano, M.C. Deblock, K.M. Hindi, S. Durmus, M.J. Panzner, C.A. Tessier, W. J. Youngs, Synthesis and anticancer properties of gold (I) and silver (I) N-heterocyclic carbene complexes, J. Organomet. Chem. 696 (5) (2011) 1066–1071, https://doi.org/10.1016/j.jorganchem.2010.10.054.
[10] M.T. Chen, B. Landers, O. Navarro, Well-defined (N-heterocyclic carbene)-Ag(i) complexes as catalysts for A 3 reactions, Org. Biomol. Chem. 10 (11) (2012) 2206–2208, https://doi.org/10.1039/c2ob06900h.
[11] S.D. Düşünceli, D. Ayaz, E. Üstün, S. Günal, N. Özdemir, M. Dinçer, İ. Özdemir, Synthesis, antimicrobial properties, and theoretical analysis of benzimidazole-2-ylidene silver(I) complexes, J. Coord. Chem. 73 (13) (2020) 1967–1986, https://doi.org/10.1080/00958972.2020.1812587.
[12] I. Slimani, et al., Novel n-heterocyclic n carbene silver(I) complexes: Synthesis, structural characterization, antimicrobial and cytotoxicity potential studies, J. Braz. Chem. Soc. 31 (10) (2020) 2058–2070, https://doi.org/10.21577/0103-5053.20200107.
[13] M. Kaloğlu, N. Kaloğlu, İ. Özdemir, S. Günal, İ. Özdemir, Novel benzimidazol-2-ylidene carbene precursors and their silver(I) complexes: Potential antimicrobial agents, Bioorg. Med. Chem. 24 (16) (2016) 3649–3656, https://doi.org/10.1016/j.bmc.2016.06.004.
[14] N. Kaloğlu, İ. Özdemir, S. Günal, İ. Özdemir, Synthesis and antimicrobial activity of bulky 3,5-di-tert-butyl substituent-containing silver–N-heterocyclic carbene complexes, Appl. Organomet. Chem. 31 (11) (2017) 1–10, https://doi.org/10.1002/aoc.3803.
[15] D. Bourissou, O. Guerret, F.P. Gabbaï, G. Bertrand, Stable Carbenes, Chem. Rev. 100 (1) (2000) 39–91, https://doi.org/10.1021/cr940472u.
[16] W.A. Herrmann, ChemInform Abstract: N-Heterocyclic Carbenes. Part 31. N-Heterocyclic Carbenes: A New Concept in Organometallic Catalysis, ChemInform 33 (32) (2002) no–no, https://doi.org/10.1002/chin.200232255.
[17] S. Díez-González, S.P. Nolan, Stereoelectronic parameters associated with N-heterocyclic carbene (NHC) ligands: A quest for understanding, Coord. Chem. Rev. 251 (5-6) (2007) 874–883, https://doi.org/10.1016/j.ccr.2006.10.004.
[18] G. Anantharaman, K. Elango, Synthesis of imidazolium/benzimidazolium salts and the preparation of silver(I) complex of bis-benzimidazolium dibromide, Synth. React. Inorg., Met.-Org., Nano-Met. Chem. 37 (9) (2007) 719–723, https://doi.org/10.1080/15533170701674959.
[19] J.C. Garrison, W.J. Youngs, "Ag (I) N-Heterocyclic Carbene Complexes : Synthesis, Structure, and Application", I (2005) 3978–4008.
[20] K.J. OBrien, L. Li (Eds.), Rightful Resistance in Rural China, Cambridge University Press, Cambridge, 2006.
[21] S. Cie, X-area (version 1.18) and X-red32 (version 1.04), Darmstadt, Germany, 2002.
[22] L. Palatinus, G. Chapuis, SUPERFLIP–a computer program for the solution of crystal structures by charge flipping in arbitrary dimensions, J. Appl. Crystallogr. 40 (4) (2007) 786–790.
[23] D. Kratzert, J.J. Holstein, I. Krossing, DSR: enhanced modelling and refinement of disordered structures with SHELXL, J. Appl. Crystallogr. 48 (3) (2015) 933–938.
[24] O.V. Dolomanov, L.J. Bourhis, R.J. Gildea, J. a. K. Howard and H. Puschmann, J. Appl. Crystallogr 42 (2009) 339–341.
[25] M.C. Arendrup, M. Cuenca-Estrella, C. Lass-Flörl, W. Hope, EUCAST-AFST,, EUCAST technical note on the EUCAST definitive document EDef 7.2: method for the determination of broth dilution minimum inhibitory concentrations of antifungal agents for yeasts EDef 7.2 (EUCAST-AFST), Clin. Microbiol. Infect. 18 (7) (2012) E246–E247.
[26] C.L.S. Institute-Clsl, Methods for dilution antimicrobial susceptibility tests for bacteria that grow aerobically; Approved standard–, M07–A9, Clinical and Laboratory Standards Institute Wayne, PA, 2015.
[27] R. Sabouraud, Contribution a l'etude de la trichophytie humaine. Etude clinique, microscopique et bacterioloqique sur la pluralité des trichophytons de l'homme, Ann. Dermatol. Syphil 3 (1892) 1061–1087.
[28] J. Sambrook, D.W. Russell, "Molecular cloning: a laboratory manual., Cold Spring Harbor Laboratory Press", Cld Spring Harbor, NY 502 (2001) 2001.
[29] S. Stepankova, K. Komers, Cholinesterases and cholinesterase inhibitors, Curr. Enzym. Inhib. 4 (4) (2008) 160–171.
[30] F. Mao, J. Li, H. Wei, L. Huang, X. Li, Tacrine–propargylamine derivatives with improved acetylcholinesterase inhibitory activity and lower hepatotoxicity as a potential lead compound for the treatment of Alzheimer's disease, J. Enzyme Inhib. Med. Chem. 30 (6) (2015) 995–1001.
[31] S. Saha, R. Verma, Inhibitory potential of traditional herbs on α-amylase activity, Pharm. Biol. 50 (3) (2012) 326–331.
[32] D. Varma, D. Sen, Role of the unfolded protein response in the pathogenesis of Parkinson's disease, Acta Neurobiol Exp (Wars) 75 (1) (2015) 1–26.
[33] I.K. Rhee, M. van de Meent, K. Ingkaninan, R. Verpoorte, Screening for acetylcholinesterase inhibitors from Amaryllidaceae using silica gel thin-layer chromatography in combination with bioactivity staining, J. Chromatogr. A 915 (1-2) (2001) 217–223.
[34] G.L. Ellman, K.D. Courtney, V. Andres, R.M. Featherstone, A new and rapid colorimetric determination of acetylcholinesterase activity, Biochem. Pharmacol. 7 (2) (1961) 88–95.
[35] S.P. de Souza, L.L.S. Pereira, A.A. Souza, C.D. dos Santos, Inhibition of pancreatic lipase by extracts of baccharis trimera: Evaluation of antinutrients and effect on glycosidases, Brazilian Journal of Pharmacognosy 21 (3) (2011) 450–455, https://doi.org/10.1590/S0102-695X2011005000049.
[36] B.C.S. Santos, A.S. Pires, Célia.H. Yamamoto, M.R.C. Couri, A.G. Taranto, M. S. Alves, A.Lúcia.dos.S.de.M. Araújo, O.V. de Sousa, Methyl chavicol and its synthetic analogue as possible antioxidant and antilipase agents based on the in vitro and in silico assays, Oxid. Med. Cell. Longevity 2018 (2018) 1–11, https://doi.org/10.1155/2018/2189348.

[37] G. Zengin, C. Sarikurkcu, A. Aktumsek, R. Ceylan, O. Ceylan, A comprehensive study on phytochemical characterization of Haplophyllum myrtifolium Boiss. endemic to Turkey and its inhibitory potential against key enzymes involved in Alzheimer, skin diseases and type II diabetes, Ind. Crops Prod. 53 (2014) 244–251.
[38] J. Cheung, E.N. Gary, K. Shiomi, T.L. Rosenberry, Structures of human acetylcholinesterase bound to dihydrotanshinone i and territrem B show peripheral site flexibility, ACS Med. Chem. Lett. 4 (11) (2013) 1091–1096, https://doi.org/10.1021/ml400304w.
[39] M. Wandhammer, E. Carletti, M. Van der Schans, E. Gillon, Y. Nicolet, P. Masson, M. Goeldner, D. Noort, F. Nachon, Structural study of the complex stereoselectivity of human butyrylcholinesterase for the neurotoxic V-agents, J. Biol. Chem. 286 (19) (2011) 16783–16789, https://doi.org/10.1074/jbc.M110.209569.
[40] R.G. Demmak, S. Bordage, A. Bensegueni, N. Boutaghane, T. Hennebelle, E. H. Mokrani, S. Sahpaz, Chemical constituents from solenostemma argel and their cholinesterase inhibitory activity, Nat. Prod. Sci. 25 (2) (2019) 115, https://doi.org/10.20307/nps.2019.25.2.115.
[41] P.P. Wizard, Epik version 2.0, Impact version 5.5, Prime version 2.1, Schrödinger, LLC, New York (NY), 2009.
[42] I. Boualia, C. Derabli, R. Boulcina, C. Bensouici, M. Yildirim, A. Birinci Yildirim, E. H. Mokrani, A. Debache, Synthesis, molecular docking studies, and biological evaluation of novel alkyl bis(4-amino-5-cyanopyrimidine) derivatives, Arch. Pharm. 352 (11) (2019) 1900027, https://doi.org/10.1002/ardp.v352.1110.1002/ardp.201900027.
[43] L. L. C. Schrödinger, "The PyMOL molecular graphics system, version 1.8." November, 2015.
[44] E.H. Mokrani, A. Bensegueni, L. Chaput, C. Beauvineau, H. Djeghim, L. Mouawad, Identification of New Potent Acetylcholinesterase Inhibitors Using Virtual Screening and in vitro Approaches, Mol. Inf. 38 (5) (2019) 1–10, https://doi.org/10.1002/minf.201800118.
[45] G. Jones, P. Willett, R.C. Glen, Molecular recognition of receptor sites using a genetic algorithm with a description of desolvation, J. Mol. Biol. 245 (1) (1995) 43–53.
[46] L.L.C. Schrodinger, The PyMOL molecular graphics system, Version 1 (5) (2010).
[47] F.H. Allen, O. Kennard, D.G. Watson, L. Brammer, A.G. Orpen, R. Taylor, Tables of bond lengths determined by X-ray and neutron diffraction. Part 1. Bond lengths in organic compounds, Journal of the Chemical Society, Perkin Transactions 2 (12) (1987) S1–S19.
[48] P. De Fremont, et al., Synthesis of well-defined N-heterocyclic carbene silver (I) complexes, Organometallics 24 (26) (2005) 6301–6309.
[49] A. Bondi, van der Waals volumes and radii, The Journal of physical chemistry 68 (3) (1964) 441–451.
[50] C. Topf, C. Hirtenlehner, U. Monkowius, Synthesis and characterization of silver (I), gold (I), and gold (III) complexes bearing a bis-dialkylamino functionalized N-heterocyclic carbene, J. Organomet. Chem. 696 (20) (2011) 3274–3278.
[51] Y.-M. Liu, et al., Synthesis and characterization of para-pyridine linked NHC palladium complexes and their studies for the Heck-Mizoroki coupling reaction, Dalton Trans. 41 (24) (2012) 7382–7389.
[52] J. Mormul, M. Steimann, C. Maichle-Mössmer, U. Nagel, Chiral Transition-Metal Complexes of Phenanthro-Annulated N-Heterocyclic Carbenes-Synthesis and Reactivity, Eur. J. Inorg. Chem. 2013 (19) (2013) 3421–3428.
[53] Q. Li, X. Li, J. Yang, H.-B. Song, L.-F. Tang, Synthesis and structural characterization of N-heterocyclic carbene silver complexes derived from N-ferrocenylmethyl-N′-(pyridylmethyl)imidazolium iodides, Polyhedron 59 (2013) 29–37, https://doi.org/10.1016/j.poly.2013.04.032.
[54] Q.-X. Liu, et al., Structures of NHC Hg (II) and Ag (I) complexes and selective recognition of nitrate anion, CrystEngComm 17 (6) (2015) 1358–1373.
[55] R.A. Haque, P.O. Asekunowo, M.R. Razali, "N HC – Silver (I) Complexes as Chemical Nucleases; Synthesis, Crystal Structures, and Antibacterial Studies" 25 (3) (2014) 194–204, https://doi.org/10.1002/hc.
[56] R.A. Haque, S.Y. Choo, S. Budagumpi, A.-A. Abdullah, M.B. Khadeer Ahamed, A.M. S. Abdul Majid, "Synthesis, crystal structures, characterization and biological studies of nitrile- functionalized silver (I) N-heterocyclic carbene complexes The School of Chemical Sciences, Universiti Sains Malaysia, 11800 USM, Penang, Centre for Nano and Material Sciences, Jain University, Jain Global Campus, Bangalore The School of Biological Sciences, Universiti Sains Malaysia, 11800 USM, Penang, EMAN Research and Testing Laboratory, The School of Pharmaceutical Sciences, The School of Chemical Sciences", INORGANICA CHIMICA ACTA, no, I 433 (2015) 35–44, https://doi.org/10.1016/j.ica.2015.04.023.
[57] A. Majid, SC, no. I. Elsevier B.V., 2015.
[58] O. Trott, A.J. Olson, AutoDock Vina: improving the speed and accuracy of docking with a new scoring function, efficient optimization, and multithreading, J. Comput. Chem. 31 (2) (2010) 455–461.